

Single-index Semiparametric Transformation Cure Models with Interval-censored Data

Xiaoru Huang¹, Tonghui Yu², Xiaoyu Liu^{1*}

¹ School of Economics, Jinan University, Guangzhou, China

² International Center for Interdisciplinary Statistics, School of Mathematics, Harbin Institute of Technology, Harbin, China

Abstract

Interval-censored data commonly arise in medical studies when the event time of interest is only known to lie within an interval. In the presence of a cure subgroup, conventional mixture cure models typically assume a logistic model for the uncure probability and a proportional hazards model for the susceptible subjects. However, in practice, the assumptions of parametric form for the uncure probability and the proportional hazards model for the susceptible may not always be satisfied. In this paper, we propose a class of flexible single-index semiparametric transformation cure models for interval-censored data, where a single-index model and a semiparametric transformation model are utilized for the uncured and conditional survival probability, respectively, encompassing both the proportional hazards cure and proportional odds cure models as specific cases. We approximate the single-index function and cumulative baseline hazard functions via the kernel technique and splines, respectively, and develop a computationally feasible expectation-maximisation (EM) algorithm, facilitated by a four-layer gamma-frailty Poisson data augmentation. Simulation studies demonstrate the satisfactory performance of our proposed method, compared to the spline-based approach and the classical logistic-based mixture cure models. The application of the proposed methodology is illustrated using the Alzheimer's dataset.

Key words: Cure model; Semiparametric transformation model; Data augmentation; EM algorithm; Interval censoring

1 Introduction

The conventional survival analysis assumes that all study subjects are susceptible to the event of interest. However, in many clinical trials, a proportion of subjects may be cured of a specific

* Corresponding author.

E-mail address: xyliu0075@jnu.edu.cn .

event. For instance, in the progression of Alzheimer’s disease (AD), a fraction of the patients diagnosed with mild cognitive impairment (MCI), which is recognized as a transitional stage, may never convert to AD. Identifying the risk factors associated with the duration time from MCI to the onset of AD is essential for early prognosis and proper clinical intervention(Oulhaj et al., 2009; Scolas et al., 2016). Moreover, the exact AD conversion time is typically known to have occurred between two consecutive visits since the patients underwent regular follow-up assessments to monitor the onset of AD (Scolas et al., 2016). Disregarding these features of survival data may lead to biases, and a more accurate approach that incorporates the cure fraction with interval censoring is required.

Literature on cure survival data mainly consists of two classes of models: the mixture cure model (Boag, 1949) and the proportional time cure model (Tsodikov et al., 1996). The mixture cure model, which posits that a population’s survival function comprises two components: the survival function of susceptible subjects (latency) and the probability of being uncured (incidence), has been investigated intensively for right censored data (Kuk and Chen, 1992; Sy and Taylor, 2000; Peng and Dear, 2000; Lu and Ying, 2004; Fang et al., 2005; Mao and Wang, 2010). In the context of interval censoring, most of the literature concentrates on assessing the impact of covariates on the conditional survival function of susceptible subjects using conventional survival models. These include the proportional hazards (PH) model (Kim and Jhun, 2008; Ma, 2009, 2010), additive hazard model (Wang et al., 2021), accelerated failure time models (Lam and Xue, 2005), generalized odds rate models (Zhou et al., 2018), semiparametric transformation models (Chen et al., 2019) and generalized accelerated failure time models (Liu and Xiang, 2021). While various survival models have been employed to analyze the latency component, relatively few studies have explored the incidence.

For the incidence, the association of the risk factors with the probability of being uncured is usually modelled via the logistic regression or log-log link function(Kuk and Chen, 1992; Sy and Taylor, 2000; Lam et al., 2005). While the logistic model is easy to implement and allows for straightforward interpretation, its rigorous parametric assumptions may be inappropriate for modelling uncured probabilities in some practical contexts. To relax the parametric assumption and enhance flexibility, nonparametric and semiparametric models have been explored. Wang et al. (2012) considered the nonparametric smoothing spline analysis of variance

(ANOVA) model, which was extended by Xu and Peng (2014) and López-Cheda et al. (2017). Xie and Yu (2021) and Aselisewine and Pal (2023) investigated machine learning techniques for incidence modelling, including neural network estimators and decision tree-based classifiers. Most existing literature has focused primarily on right-censored data, with limited research available on interval-censored data.

The fully nonparametric models mentioned above lack interpretability and may encounter the “curse of dimensionality” issue when the dimension of the covariates is large. Therefore, a more flexible semiparametric single-index model is required. The model is computationally tractable with numerous covariates and allows for assessing the relative importance of covariates by examining the absolute values of their coefficients. The single-index approach has been investigated in the context of survival data (Lu et al., 2006; Sun et al., 2008; Gorst-Rasmussen and Scheike, 2013). Recently, Amico et al. (2019) introduced the single-index model for incidence, assuming a proportional hazards model on the latency component with right-censored data. Extending this work, Lee et al. (2024) proposed two single-index modelling frameworks for both the incidence and latency components retaining the proportional hazards assumption for the latter. However, these methodologies are limited to right-censored data. Unlike right-censoring, interval-censored data, where the exact event time is only known to lie within an interval, inherently provides less information and introduces both theoretical and computational challenges (Sun, 2006). For instance, in right-censored settings, the partial likelihood function (which eliminates the baseline hazard) and the martingale process theory are standard tools for regression parameter estimation and inference. Such approaches, however, are generally inapplicable to interval-censored data. Furthermore, the imposition of a proportional hazards constraint on the latency may limit the model’s flexibility and practical applicability.

In this paper, we developed a flexible single-index semiparametric transformation mixture cure model for interval-censored data (SMCI) to address potential non-monotonic and non-logistic patterns in the incidence while providing a more general survival function for the latency. The kernel smoothing approach is employed to estimate the unknown link function of the incidence, and the spline technique is utilized to approximate the unspecified, increasing function within the transformation model in the latency. Conditional on the frailty variable induced by

a transformation model, we propose a four-layer data augmentation procedure and develop an expectation-maximization (EM) algorithm for parameter estimation. For comparison, we also consider the splines approach for the incidence. Additionally, we provide results about the model identifiability.

The remainder of the paper is structured as follows. Section 2 presents a single-index mixture cure model for interval-censored data and discusses the model identifiability. Section 3 introduces the four-layer data augmentation procedure and the detailed EM algorithm. The finite sample performance and real data analysis are illustrated in Section 4 and 5, respectively. Section 6 provides a summary and discussion of the entire text. All technical proofs are provided in the Appendix.

2 Data, Model and Likelihood

2.1 Model and Likelihood

Let T be a nonnegative random variable representing the event time of interest. To account for the presence of the cure subgroup in the population, we introduce the latent cure indicator B , with $B = 1$ if the individual is susceptible, and 0 otherwise. The survival time T can then be expressed as $T = (1 - B)\infty + B \times T^*$, where T^* is the survival function of susceptible subjects. Under mixed case interval censoring, denote (V_1, \dots, V_K) the random sequence of observation times, with K being the random number of observation times. Write $\tilde{V} = (V_0, V_1, \dots, V_K, V_{K+1})$, where $V_0 = 0$ and $V_{K+1} = \infty$. Assume (L, R) be the smallest interval that contains T , i.e., $L = \max\{V_k : V_k < T\}$ and $R = \min\{V_k : V_k \geq T\}$. Note that $L = 0$ if the subject is left-censored, and $R = \infty$ if the subject is right-censored. Define interval censoring indicators as $\delta_L = \mathbf{1}(L = 0)$, $\delta_I = \mathbf{1}(0 < L < R < \infty)$ and $\delta_R = \mathbf{1}(R = \infty)$, where $\mathbf{1}(\cdot)$ is the indicator function. Let \mathbf{X} and \mathbf{Z} be d_1 -dimensional and d_2 -dimensional vectors of covariates associated with the cure fraction and the event occurrence time of a susceptible group, respectively. Note that \mathbf{X} and \mathbf{Z} may overlap or differ.

Under the mixture cure models, the (improper) conditional survival function of T is defined as

$$S(t|\mathbf{X}, \mathbf{Z}) = 1 - p(\mathbf{X}) + p(\mathbf{X})S_u(t|\mathbf{Z}), \quad (1)$$

where the incidence component $p(\mathbf{X})$ denotes the uncure probability, and the latency component $S_u(\cdot|\mathbf{Z})$ represents the survival function of uncured groups.

In the latency part, we assume the semiparametric transformation model for individuals susceptible to the event, that is

$$S_u(t|\mathbf{Z}) = \exp \left[-G \left\{ \exp(\boldsymbol{\beta}^\top \mathbf{Z}) \Lambda(t) \right\} \right], \quad (2)$$

where $\boldsymbol{\beta}$ is a vector of regression parameters, $\Lambda(\cdot)$ is an unknown increasing function with $\Lambda(0) = 0$ and $G(\cdot)$ is a specific monotone transformation function. Model (2) is a class of flexible semiparametric models, including the linear transformation model (Chen et al., 2002) and the generalized odds rate model (Zhou et al., 2018). We consider a class of frailty-induced transformation function for $G(x)$, that is $G(x) = -\log \left\{ \int_0^\infty \exp(-x\xi) f(\xi) d\xi \right\}$, where $f(\xi)$ is the density function of the frailty ξ . The choice of the gamma density with mean 1 and variance r for $f(\xi)$ yields the class of logarithmic transformations $G(x) = r^{-1} \log(1 + rx)$ with $r \geq 0$, which includes the proportional hazards model ($r = 0$), and the proportional odds model ($r = 1$) as special cases (Zeng and Lin, 2006; Zeng et al., 2016).

In the incidence part, we consider a semiparametric single-index model in terms of the susceptible probability

$$p(\mathbf{X}) = g(\boldsymbol{\gamma}^\top \mathbf{X}), \quad (3)$$

where $\boldsymbol{\gamma} = (\gamma_1, \dots, \gamma_{d_1})^\top$ is a vector of regression coefficients and $g(\cdot)$ is an unknown smooth link function (monotone or non-monotone) with values between 0 and 1. Model (3) provides more flexibility compared to conventional parametric models. Specifically, it allows us to explore the various cure frameworks for incidence, including the logistic regression and complementary log-log model defined by $g(x) = \{1 + \exp(-x)\}^{-1}$ and $g(x) = \{1 - \exp\{-\exp(x)\}\}^{-1}$, respectively (Sy and Taylor, 2000; Lam et al., 2005). With \mathbf{X} being univariate, model (3) reduces to the nonparametric model as described by Xu and Peng (2014) and López-Cheda et al. (2017). Furthermore, it avoids the curse of dimensionality associated with completely nonparametric models while maintaining ease of interpretation through its structured approach (Horowitz, 2009).

Assume that T and (\tilde{V}, K) are independent conditional on covariates (\mathbf{X}, \mathbf{Z}) . A ran-

dom sample of size n comprises $\mathcal{O} = \{(L_i, R_i, \delta_{L_i}, \delta_{I_i}, \delta_{R_i}, \mathbf{X}_i, \mathbf{Z}_i), (i = 1, \dots, n)\}$. Let $\boldsymbol{\theta} = (\boldsymbol{\gamma}, \boldsymbol{\beta}, g, \Lambda)^\top$ be the set of unknown parameters, then the likelihood function takes the form

$$L(\boldsymbol{\theta}|\mathcal{O}) = \prod_{i=1}^n [1 - S(R_i|\mathbf{X}_i, \mathbf{Z}_i)]^{\delta_{R_i}} [S(L_i|\mathbf{X}_i, \mathbf{Z}_i) - S(R_i|\mathbf{X}_i, \mathbf{Z}_i)]^{\delta_{I_i}} S(L_i|\mathbf{X}_i, \mathbf{Z}_i)^{\delta_{L_i}}.$$

By substituting $S(t|\mathbf{X}, \mathbf{Z})$ with (1) and plugging (2) into the likelihood function, we have

$$\begin{aligned} L(\boldsymbol{\theta}|\mathcal{O}) &= \prod_{i=1}^n p(\mathbf{X}_i)^{1-\delta_{R_i}} \int_{\xi_i} [1 - \exp\{-\xi_i \exp(\boldsymbol{\beta}^\top \mathbf{Z}_i) \Lambda(R_i)\}]^{\delta_{L_i}} \\ &\quad \times [\exp\{-\xi_i \exp(\boldsymbol{\beta}^\top \mathbf{Z}_i) \Lambda(L_i)\} - \exp\{-\xi_i \exp(\boldsymbol{\beta}^\top \mathbf{Z}_i) \Lambda(R_i)\}]^{\delta_{I_i}} \\ &\quad \times [1 - p(\mathbf{X}_i) + p(\mathbf{X}_i) \exp\{-\xi_i \exp(\boldsymbol{\beta}^\top \mathbf{Z}_i) \Lambda(L_i)\}]^{\delta_{R_i}} f(\xi_i) d\xi_i. \end{aligned} \quad (4)$$

2.2 Identifiability of the Model

Let $\boldsymbol{\gamma}_0$, $\boldsymbol{\beta}_0$, g_0 , and Λ_0 be the true parameter values. Denote by \mathcal{X} and \mathcal{Z} the support of \mathbf{X} and \mathbf{Z} , respectively. We impose the following conditions for model identifiability

- (A1) The function g_0 is differentiable and not constant on the support of $\boldsymbol{\gamma}_0^\top \mathbf{X}$.
- (A2) The covariate vector \mathbf{X} is continuous and does not contain an intercept. The support \mathcal{X} is not contained in any proper linear subspace of \mathbb{R}^{d_1} .
- (A3) The parameter $\boldsymbol{\gamma}_0 \in \mathcal{A}_\gamma$, where $\mathcal{A}_\gamma = \{(\gamma_1, \gamma_2, \dots, \gamma_{d_1}) \mid \sum_{j=1}^{d_1} \gamma_j^2 = 1, \gamma_1 > 0 \text{ or } \gamma_1 = 1\}$.
- (A4) The covariate vector \mathbf{Z} does not contain an intercept, and the support \mathcal{Z} is not contained in any proper linear subspace of \mathbb{R}^{d_2} .
- (A5) The transformation function G is continuously differentiable on $[0, \infty)$ with $G(0) = 0$, $G'(x) > 0$ and $G(\infty) = \infty$.
- (A6) For all \mathbf{X} , $0 < g_0(\boldsymbol{\gamma}_0^\top \mathbf{X}) < 1$. $\lim_{t \rightarrow \infty} S_u(t|\mathbf{Z}) = 0$ for all \mathbf{Z} , indicating the latency function is proper.

Assumptions (A1)-(A3) are needed to identify the single-index model for the incidence (Theorem 2.1 in Horowitz (2009) and Amico et al. (2019)). Assumptions (A4)-(A5) are required for the identifiability of the latency model. (A6) imposes mild conditions to ensure separate identifiability of the incidence and latency components.

Proposition 1. Under (A1)-(A6), the model given by (1), (2), and (3) is identifiable.

The proof of Proposition 1 is given in the Appendix. Note that the above assumptions apply when \mathbf{X} is a continuous random vector. For \mathbf{X} that contains both continuous and discrete components, the following additional conditions must hold:

- (A7) Varying the values of the discrete components must not divide the support of $\gamma_0^\top \mathbf{X}$ into disjoint subsets.
- (A8) The function g_0 is not periodic.

3 Estimation Procedure

The involvement of the integral in the transformation model makes it challenging to directly maximize the intractable likelihood function (4). Therefore, we propose a four-layer data augmentation procedure and develop an expectation-maximization (EM) algorithm for parameter estimation.

3.1 Data Augmentation

The first layer simplifies the likelihood function by introducing a latent cure indicator B_i for subject i . Assume $B_i \sim \text{Bern}(p(\mathbf{X}_i))$, where $\text{Bern}(p(\mathbf{X}_i))$ denotes the Bernoulli distribution with parameter $p(\mathbf{X}_i)$, representing the probability of being uncured. Note that $B_i = 1$ when $\delta_{R_i} = 0$ for data that are not right-censored. For subject i with $\delta_{R_i} = 1$, the contribution to the likelihood is $1 - p(\mathbf{X}_i)$ if $B_i = 0$, and $p(\mathbf{X}_i)S_u(L_i|\mathbf{Z}_i)$ if $B_i = 1$. Utilizing the relationship $(1 - B_i)\delta_{R_i} = 1 - B_i$, the augmented data likelihood function can be written as

$$\begin{aligned} L_1(\boldsymbol{\theta}|\mathcal{O}, \mathbf{B}) &= \prod_{i=1}^n p(\mathbf{X}_i)^{B_i} [1 - p(\mathbf{X}_i)]^{1-B_i} \int_{\xi_i} [1 - \exp\{-\xi_i \exp(\boldsymbol{\beta}^\top \mathbf{Z}_i) \Lambda(R_i)\}]^{\delta_{L_i}} \\ &\quad \times [\exp\{-\xi_i \exp(\boldsymbol{\beta}^\top \mathbf{Z}_i) \Lambda(L_i)\} - \exp\{-\xi_i \exp(\boldsymbol{\beta}^\top \mathbf{Z}_i) \Lambda(R_i)\}]^{\delta_{I_i}} \\ &\quad \times \exp\{-\delta_{R_i} B_i \xi_i \exp(\boldsymbol{\beta}^\top \mathbf{Z}_i) \Lambda(L_i)\} f(\xi_i) d\xi_i. \end{aligned}$$

In the second layer, we introduce the latent variable ξ_i . Conditional on ξ_i and B_i , the augmented likelihood function then tasks the form

$$\begin{aligned} L_2(\boldsymbol{\theta}|\mathcal{O}, \mathbf{B}, \boldsymbol{\xi}) &= \prod_{i=1}^n p(\mathbf{X}_i)^{B_i} [1 - p(\mathbf{X}_i)]^{1-B_i} [1 - \exp\{-\xi_i \exp(\boldsymbol{\beta}^\top \mathbf{Z}_i) \Lambda(R_i)\}]^{\delta_{L_i}} \\ &\quad \times [\exp\{-\xi_i \exp(\boldsymbol{\beta}^\top \mathbf{Z}_i) \Lambda(L_i)\} - \exp\{-\xi_i \exp(\boldsymbol{\beta}^\top \mathbf{Z}_i) \Lambda(R_i)\}]^{\delta_{I_i}} \\ &\quad \times \exp\{-\delta_{R_i} B_i \xi_i \exp(\boldsymbol{\beta}^\top \mathbf{Z}_i) \Lambda(L_i)\} f(\xi_i). \end{aligned}$$

In the third layer, we introduced nonhomogenous Poisson latent variables to construct the augmented likelihood function. The technique leads to simplified likelihood framework and is commonly utilized for interval-censored data (Zeng et al., 2016; Zhou et al., 2018). Specifically, we define two Poisson random variables Y_i and W_i with means given by $\lambda_i \xi_i$ and $\omega_i \xi_i$, where $\lambda_i = \exp(\boldsymbol{\beta}^\top \mathbf{Z}_i)[\delta_{L_i} \Lambda(R_i) + \delta_{I_i} \Lambda(L_i)]$ and $\omega_i = \exp(\boldsymbol{\beta}^\top \mathbf{Z}_i)\{\delta_{I_i}[\Lambda(R_i) - \Lambda(L_i)] + \delta_{R_i} \Lambda(L_i)\}$. Clearly, Y_i and W_i are independent conditional on ξ_i and \mathbf{Z}_i . Define $Y_i \equiv 0$ if $Y_i \sim \text{Poisson}(0)$. Within this framework, $Y_i > 0$ and $W_i = 0$ if T_i is left-censored, $Y_i = 0$ and $W_i > 0$ if T_i is interval-censored, $Y_i = W_i = 0$ if T_i is right-censored. By leveraging these Poisson latent variables, the augmented likelihood function can be formulated as

$$\begin{aligned} L_3(\boldsymbol{\theta}|\mathcal{O}, \mathbf{B}, \boldsymbol{\xi}, \mathbf{Y}, \mathbf{W}) &= \prod_{i=1}^n p(\mathbf{X}_i)^{B_i} \{1 - p(\mathbf{X}_i)\}^{1-B_i} \left\{ \frac{(\lambda_i \xi_i)^{Y_i}}{Y_i!} e^{-\lambda_i \xi_i} \right\}^{\delta_{L_i}} \\ &\quad \times \left\{ \frac{(\omega_i \xi_i)^{W_i}}{W_i!} e^{-(\omega_i + \lambda_i) \xi_i} \right\}^{\delta_{I_i}} \exp(-\delta_{R_i} B_i \omega_i \xi_i) f(\xi_i), \end{aligned}$$

under the constraint $\delta_{L_i} I(Y_i > 0) + \delta_{I_i} I(W_i > 0) + \delta_{R_i} = 1$ for $i = 1, \dots, n$.

We utilize the monotone splines technique defined in Ramsay (1988) to approximate the unspecified increasing function $\Lambda(\cdot)$ in the transformation model. Specifically, we approximate $\Lambda(\cdot)$ with a linear combination of basis I-splines:

$$\Lambda(t) = \sum_{l=1}^k \eta_l b_l(t), \quad (5)$$

where $\{b_l(t)\}$ is a set of I-spline basis functions ranging from 0 to 1, $\boldsymbol{\eta} = (\eta_1, \dots, \eta_k)^\top$ are non-negative coefficients to ensure the monotonicity of $\Lambda(\cdot)$, and k is the number of basis I-splines determined by knot placement and the degrees of splines. This spline-based formulation offers a computationally efficient alternative to step-function approximations (Zeng et al., 2016) by

reducing the parameter dimensionality, while simultaneously providing a smooth estimate of the hazard rate. As a general guideline, using an order of 2 (quadratic) or 3 (cubic) with 5 to 15 knots offers adequate smoothness and sufficient flexibility. Knot placement can be either evenly spaced or determined by percentiles, based on our extensive experience.

In the fourth layer, we consider further data augmentation to derive a closed-form update for the coefficients of the monotone spline basis, utilizing the additivity property of Poisson random variables and the linear form of $\Lambda(t)$ in (5). Decompose both Y_i and W_i as a sum of k independent Poisson random variables, $Y_i = \sum_{l=1}^k Y_{il}$ and $W_i = \sum_{l=1}^k W_{il}$, where $Y_{il} \sim \mathcal{P}\{\eta_l \exp(\boldsymbol{\beta}^\top \mathbf{Z}_i)[\delta_{L_i} b_l(R_i) + \delta_{I_i} b_l(L_i)]\xi_i\}$ and $W_{il} \sim \mathcal{P}\{\eta_l \exp(\boldsymbol{\beta}^\top \mathbf{Z}_i)\{\delta_{I_i}[b_l(R_i) - b_l(L_i)] + \delta_{R_i} b_l(L_i)\}\xi_i\}$ for $l = 1, \dots, k$, where \mathcal{P} denotes the Poisson probability mass function. Let $\lambda_{il} = \eta_l \exp(\boldsymbol{\beta}^\top \mathbf{Z}_i)[\delta_{L_i} b_l(R_i) + \delta_{I_i} b_l(L_i)]$ and $\omega_{il} = \eta_l \exp(\boldsymbol{\beta}^\top \mathbf{Z}_i)\{\delta_{I_i}[b_l(R_i) - b_l(L_i)] + \delta_{R_i} b_l(L_i)\}$. The final complete likelihood function based on ξ_i 's, B_i 's, Y_{il} 's and W_{il} 's has the form

$$L_4(\boldsymbol{\theta} | \mathcal{O}, \mathbf{B}, \boldsymbol{\xi}, \mathbf{Y}, \mathbf{W}) = \prod_{i=1}^n p(\mathbf{X}_i)^{B_i} \{1 - p(\mathbf{X}_i)\}^{1-B_i} \left[\prod_{l=1}^k \left\{ \frac{(\lambda_{il}\xi_i)^{Y_{il}}}{Y_{il}!} e^{-\lambda_{il}\xi_i} \right\}^{\delta_{L_i}} \right. \\ \left. \times \left\{ \frac{(\omega_{il}\xi_i)^{W_{il}}}{W_{il}!} e^{-(\omega_{il} + \lambda_{il})\xi_i} \right\}^{\delta_{I_i}} \exp(-\delta_{R_i} B_i \omega_{il} \xi_i) \right] f(\xi_i), \quad (6)$$

under the constraint $\delta_{L_i} I(\sum_{l=1}^k Y_{il} > 0) + \delta_{I_i} I(\sum_{l=1}^k W_{il} > 0) + \delta_{R_i} = 1$ for $i = 1, \dots, n$. The observed likelihood function (4) can be achieved by integrating out the latent variables \mathbf{B} , $\boldsymbol{\xi}$, Y_l 's and W_l 's in the complete likelihood function (6). The deduction of equation (6) to (4) is given in the Appendix.

3.2 Nonparametric regression for Incidence

For the nonparametric link function g , two popular techniques, spline and kernel methods, can be utilized.

The spline-based sieve approach has been extensively studied in the semiparametric models of survival data (Ding and Nan, 2011; Zhao et al., 2017; Liu and Xiang, 2021). In the single-index model, the nonparametric function g involves the parametric component $\boldsymbol{\gamma}^\top \mathbf{X}$, and thus it requires constructing the splines over intervals for a given $\boldsymbol{\gamma}$. Specifically, let $a^\gamma = \min_{1 \leq i \leq n} \{\boldsymbol{\gamma}^\top \mathbf{X}_i\}$ and $b^\gamma = \max_{1 \leq i \leq n} \{\boldsymbol{\gamma}^\top \mathbf{X}_i\}$. We approximate the link function us-

ing B-spline functions on $[a^\gamma, b^\gamma]$ for a fixed γ :

$$g(\gamma^\top \mathbf{X}) = \sum_{j=1}^m \psi_j b_j^*(\gamma^\top \mathbf{X}), \quad (7)$$

where $\{b_j^*(\cdot)\}$ represents a set of B-spline basis functions, and $\psi = (\psi_1, \dots, \psi_m)$ denotes the spline coefficients. Note that the end points of such intervals vary with different values of γ , yielding more challenges in the estimation procedure.

Alternative nonparametric techniques, such as the kernel technique, could also be used for the estimation of g . The kernel approach has been investigated for the nonparametric covariate functions (Amico et al., 2019; Wang and Yu, 2021, 2022). For a given γ , the link function $g(\cdot)$ can be obtained by the (unfeasible) leave-one-out kernel estimator (Amico et al., 2019)

$$g_{-i}(\gamma^\top \mathbf{X}_i) = \frac{\sum_{j \neq i}^n K(\frac{\gamma^\top \mathbf{X}_i - \gamma^\top \mathbf{X}_j}{h}) B_j}{\sum_{l \neq i}^n K(\frac{\gamma^\top \mathbf{X}_i - \gamma^\top \mathbf{X}_l}{h})}, \quad (8)$$

where $K(\cdot)$ is a kernel function, h is a one-dimensional bandwidth and \mathbf{B} is the latent cure status, which can be replaced by its expectation in the calculation. The bandwidth h is selected via likelihood cross-validation, with the complete procedure detailed in the simulation studies (Section 4). For an illustration, we compared the kernel estimator with the cubic B-splines estimator for the incidence part in the simulation studies.

3.3 EM Algorithm

The expectation step involves calculating $E\{\log L_c(\boldsymbol{\theta}|\mathcal{O}, \mathbf{B}, \mathbf{Y}, \mathbf{W})\}$ with respect to all latent variables \mathbf{Y} , \mathbf{W} , \mathbf{B} and $\boldsymbol{\xi}$ conditional on the observed data \mathcal{O} and the current parameter $\boldsymbol{\theta}^{(d)} = (\boldsymbol{\gamma}^{(d)}, \boldsymbol{\beta}^{(d)}, \boldsymbol{\eta}^{(d)})$. We omit all conditional arguments in the expectations henceforth for the sake of clarity; for instance, we write $E(B_i)$ instead of $E(B_i|\mathcal{O}, \boldsymbol{\theta}^{(d)})$. The objective function can be written as the sum of two parts

$$Q(\boldsymbol{\theta}, \boldsymbol{\theta}^{(d)}) = Q_1(\boldsymbol{\gamma}, \boldsymbol{\gamma}^{(d)}) + Q_2(\boldsymbol{\beta}, \boldsymbol{\eta}; \boldsymbol{\beta}^{(d)}, \boldsymbol{\eta}^{(d)}),$$

where

$$Q_1(\boldsymbol{\gamma}, \boldsymbol{\gamma}^{(d)}) = \sum_{i=1}^n E(B_i) \log[g(\boldsymbol{\gamma}^\top \mathbf{X}_i)] + [1 - E(B_i)] \log[1 - g(\boldsymbol{\gamma}^\top \mathbf{X}_i)], \quad (9)$$

$$Q_2(\boldsymbol{\beta}, \boldsymbol{\eta}; \boldsymbol{\beta}^{(d)}, \boldsymbol{\eta}^{(d)}) = \sum_{i=1}^n \sum_{l=1}^k \left\{ [\delta_{L_i} E(Y_{il}) + \delta_{I_i} E(W_{il})] (\log \eta_l + \boldsymbol{\beta}^\top \mathbf{Z}_i) \right. \\ \left. - \eta_l \exp(\boldsymbol{\beta}^\top \mathbf{Z}_i) E(\xi_i B_i) [(1 - \delta_{R_i}) b_l(R_i) + \delta_{R_i} b_l(L_i)] \right\}, \quad (10)$$

after omitting additive terms that are free of $\boldsymbol{\theta}$.

We show that the conditional expectations of the latent variables are given as:

$$E(Y_{il}) = \frac{\eta_l^{(d)} b_l(R_i) E(Y_i)}{\sum_{l=1}^k \eta_l^{(d)} b_l(R_i)}, \quad E(Y_i) = \frac{\delta_{L_i} N_{i2}^{(d)} \int_{\xi_i} \xi_i f(\xi_i) d\xi_i}{1 - \exp\{-G(N_{i2}^{(d)})\}}, \quad (11)$$

$$E(W_{il}) = \frac{\eta_l^{(d)} [b_l(R_i) - b_l(L_i)] E(W_i)}{\sum_{l=1}^k \eta_l^{(d)} [b_l(R_i) - b_l(L_i)]}, \quad (12)$$

$$E(W_i) = \frac{\delta_{I_i} (N_{i2}^{(d)} - N_{i1}^{(d)}) \exp\{-G(N_{i1}^{(d)})\} G'(N_{i1}^{(d)})}{\exp\{-G(N_{i1}^{(d)})\} - \exp\{-G(N_{i2}^{(d)})\}}, \quad (13)$$

$$E(B_i) = \delta_{L_i} + \delta_{I_i} + \frac{\delta_{R_i} p^{(d)}(\mathbf{X}_i) \exp\{-G(N_{i1}^{(d)})\}}{1 - p^{(d)}(\mathbf{X}_i) + p^{(d)}(\mathbf{X}_i) \exp\{-G(N_{i1}^{(d)})\}}, \quad (14)$$

and

$$E(\xi_i B_i) = \delta_{L_i} \frac{\int_{\xi_i} \xi_i f(\xi_i) d\xi_i - \exp\{-G(N_{i2}^{(d)})\} G'(N_{i2}^{(d)})}{1 - \exp\{-G(N_{i2}^{(d)})\}} \\ + \delta_{I_i} \frac{\exp\{-G(N_{i1}^{(d)})\} G'(N_{i1}^{(d)}) - \exp\{-G(N_{i2}^{(d)})\} G'(N_{i2}^{(d)})}{\exp\{-G(N_{i1}^{(d)})\} - \exp\{-G(N_{i2}^{(d)})\}} \\ + \delta_{R_i} \frac{p^{(d)}(\mathbf{X}_i) \exp\{-G(N_{i1}^{(d)})\} G'(N_{i1}^{(d)})}{1 - p^{(d)}(\mathbf{X}_i) + p^{(d)}(\mathbf{X}_i) \exp\{-G(N_{i1}^{(d)})\}}, \quad (15)$$

where $N_{i1}^{(d)} = \exp(\boldsymbol{\beta}^{(d)\top} Z_i) \sum_{l=1}^k \eta_l^{(d)} b_l(L_i)$, $N_{i2}^{(d)} = \exp(\boldsymbol{\beta}^{(d)\top} Z_i) \sum_{l=1}^k \eta_l^{(d)} b_l(R_i)$. The detailed derivations of the above conditional expectations are presented in the Appendix.

The maximization step finds $\boldsymbol{\theta}^{(d+1)} = \arg \max Q(\boldsymbol{\theta}, \boldsymbol{\theta}^{(d)})$, where $Q(\boldsymbol{\theta}, \boldsymbol{\theta}^{(d)}) = Q_1(\boldsymbol{\gamma}, \boldsymbol{\gamma}^{(d)}) + Q_2(\boldsymbol{\beta}, \boldsymbol{\eta}; \boldsymbol{\beta}^{(d)}, \boldsymbol{\eta}^{(d)})$.

We update $\boldsymbol{\gamma}^{(d+1)}$ by maximizing $Q_1(\boldsymbol{\gamma}, \boldsymbol{\gamma}^{(d)})$ described in Eq (9). For the kernel-based approach, the link function $g(\cdot)$ can be obtained by the leave-one-out kernel estimator (Amico et al., 2019)

$$g_{-i}(\boldsymbol{\gamma}^\top \mathbf{X}_i) = \frac{\sum_{j \neq i}^n K(\frac{\boldsymbol{\gamma}^\top \mathbf{X}_i - \boldsymbol{\gamma}^\top \mathbf{X}_j}{h}) E(B_j)}{\sum_{l \neq i}^n K(\frac{\boldsymbol{\gamma}^\top \mathbf{X}_i - \boldsymbol{\gamma}^\top \mathbf{X}_l}{h})}, \quad (16)$$

where h is a one-dimensional bandwidth. Substituting expression (16) into Eq (9) and maximizing it, we obtain the updated estimate $\boldsymbol{\gamma}^{(d+1)}$. Using $\boldsymbol{\gamma}^{(d+1)}$, we compute $g_{-i}^{(d+1)}((\boldsymbol{\gamma}^{(d+1)})^\top \mathbf{X}_i)$ with the estimator provided in Equation (16). The sieve estimator of g can be obtained in a similar way.

Setting the derivative $\frac{\partial Q_2(\boldsymbol{\beta}, \boldsymbol{\eta}; \boldsymbol{\beta}^{(d)}, \boldsymbol{\eta}^{(d)})}{\partial \eta_l} = 0$, for $l = 1, \dots, k$, we obtain the closed-form solution for η_l based on $\boldsymbol{\beta}$:

$$\eta_l(\boldsymbol{\beta}) = \frac{\sum_{i=1}^n \{\delta_{L_i} E(Y_{il}) + \delta_{I_i} E(W_{il})\}}{\sum_{i=1}^n \exp(\boldsymbol{\beta}^\top \mathbf{Z}_i) E(\xi_i B_i) \{(1 - \delta_{R_i}) b_l(R_i) + \delta_{R_i} b_l(L_i)\}}, \quad l = 1, \dots, k. \quad (17)$$

Substituting $\eta_l(\boldsymbol{\beta})$ into Eq (10) and differentiating with respect to $\boldsymbol{\beta}$, we can obtain $\boldsymbol{\beta}^{(d+1)}$ by solving the score function:

$$\sum_{i=1}^n \sum_{l=1}^k \left[\{\delta_{L_i} E(Y_{il}) + \delta_{I_i} E(W_{il})\} - \eta_l(\boldsymbol{\beta}) \exp(\boldsymbol{\beta}^\top \mathbf{Z}_i) E(\xi_i B_i) \{(1 - \delta_{R_i}) b_l(R_i) + \delta_{R_i} b_l(L_i)\} \right] \mathbf{Z}_i = 0. \quad (18)$$

The updated $\eta_l^{(d+1)} = \eta_l(\boldsymbol{\beta}^{(d+1)})$ for $l = 1, 2, \dots, k$ is determined by Eq (17).

We summarise the proposed EM algorithm for calculating estimates for $\boldsymbol{\theta}$ as follows:

Step 1. Set initial values $\boldsymbol{\theta}^{(0)} = (\boldsymbol{\gamma}^{(0)}, \boldsymbol{\beta}^{(0)}, \boldsymbol{\eta}^{(0)})$, where $\boldsymbol{\beta}^{(0)} = \mathbf{0}$, $\boldsymbol{\eta}^{(0)} = \mathbf{1}$, and $\boldsymbol{\gamma}^{(0)}$ is obtained by fitting the generalized additive model using pseudo values $1 - \delta_{R_i}$.

Step 2. In the $(d+1)$ th iteration, calculate the expectations in Eqs (11) - (15) based on $(\boldsymbol{\theta}^{(d)}, \mathcal{O})$.

Step 3. Obtain $\boldsymbol{\gamma}^{(d+1)}$ by maximizing $Q_1(\boldsymbol{\gamma}, \boldsymbol{\gamma}^{(d)})$ given in Eq (9), and calculate the Nadaraya-Watson estimator $g(\boldsymbol{\gamma}^\top \mathbf{X}_i)^{(d+1)}$ by $g_{-i}^{(d+1)}((\boldsymbol{\gamma}^{(d+1)})^\top \mathbf{X}_i)$.

Step 4. Obtain $\boldsymbol{\beta}^{(d+1)}$ by calculating the estimating equation Eq (18).

Step 5. Obtain $\eta_l^{(d+1)}$ by Eq (17) based on $\boldsymbol{\beta}^{(d+1)}$.

Step 6. Repeat Steps 2 to 5 until the convergence criterion is satisfied, obtaining the final iterative values $\hat{\boldsymbol{\theta}} = (\hat{\boldsymbol{\gamma}}, \hat{\boldsymbol{\beta}}, \hat{\boldsymbol{\eta}})$.

The initial values of $\boldsymbol{\gamma}$ are obtained using the `gam` function from R package `mgcv`, and the Newton–Raphson algorithm is employed to maximise the objective function.

We utilize the bootstrap method to estimate the asymptotic variance of the estimator for practical use. This method further facilitates the variance estimation of the cumulative baseline hazard function $\Lambda(t)$, at any fixed time point t . Alternatively, the profile likelihood technique (Murphy and Van der Vaart, 2000) and the resampling approach that generalizes the perturbing technique of Jin et al. (2003) can also be employed.

4 Simulation

Extensive simulation studies are conducted to evaluate the finite sample performance of the proposed estimators, including the SMCI model with kernel estimator (SMCI-K) and the SMCI model with spline estimator (SMCI-S). For comparison, we employ the generalized odds rate mixture cure (GORMC) model proposed by Zhou et al. (2018), which assumes a logistic regression for the incidence and a semiparametric transformation model for the latency.

For the incidence component, we consider three different scenarios. Scenario 1 employs a logistic regression model. Scenario 2 utilizes a non-logistic but monotonic link function defined as $g(u) = (1 + \tanh(1.5u^5))/2$. The third scenario posits a non-logistic model for incidence with a non-monotonic shape, expressed as $g(u) = \exp(4.8u^3 - 8u^2 + 3.2u + 0.85)/[1 + \exp(4.8u^3 - 8u^2 + 3.2u + 0.85)]$. In each scenario, we consider three covariates: $X_1 \sim \text{Unif}(-1, 2)$, $X_2 \sim N(0, 1)$ and $X_3 \sim \text{Bern}(0.5)$, and the true parameters $\boldsymbol{\gamma} = (1/\sqrt{3}, -1/\sqrt{3}, 1/\sqrt{3})^\top$, respectively. Given the incidence component $p(\mathbf{X})$, the uncured status B is generated from a Bernoulli distribution with the parameter equal to $p(\mathbf{X})$. Depending on the scenario, the cure proportion ranged from 22.6% (in Scenario 2 with $r = 2$) to 38% (in Scenario 1 with $r = 1$).

For the latency component, we generate the failure times of susceptible subjects from the transformation model

$$\Lambda_u(t|\mathbf{Z}) = G \left\{ \exp(\boldsymbol{\beta}^\top \mathbf{Z}) \Lambda(t) \right\},$$

where $G(x) = r^{-1} \log(1 + rx)$ and $\Lambda(t) = 0.5 \log(1 + t) + 0.5t^{1.5} + 0.5t^3$. We consider covariates

$Z_1 \sim \text{Unif}(0, 2)$, $Z_2 \sim \text{N}(0, 1)$ and $Z_3 \sim \text{Bern}(0.5)$, with parameters set as $\beta = (1, -1, 1)^\top$. We investigate three models for the survival function of susceptible subjects by specifying $r = 0$, 1 or 2, corresponding to the proportional hazards model, proportional odds model and the generalized odds rate model, respectively. The interval-censored data are then generated in the following way similar to that in Zhou et al. (2018). On average, there were 10–15% left-censored observations and 40–45% right-censored ones. Two sample sizes $n = 200$ and $n = 500$ are considered, and a total of 200 replicated datasets are generated for each sample size. The simulation setting is detailed in Appendix Table 5.

According to Wang et al. (2016a), we utilize 5 equally spaced knots at the percentiles with the degree of 3 for the monotone splines. We choose the Epanechnikov kernel

$$K(u) = \frac{(3 - 0.6u^2)I(u^2 \leq 5)}{4\sqrt{5}}$$

for the SMCI-K model, and select bandwidth by the likelihood cross-validation criterion. The criterion is defined as $\text{CV}^{(d+1)}(h) = \sum_1^n E(B_i) \log\{\hat{g}_{h,-i}^{(d)}(\hat{\gamma}^{(d)\top} \mathbf{X}_i)\} + (1 - E(B_i)) \log\{1 - \hat{g}_{h,-i}^{(d)}(\hat{\gamma}^{(d)\top} \mathbf{X}_i)\}$, where $\hat{g}_{h,-i}^{(d)}(\hat{\gamma}^{(d)\top} \mathbf{X}_i)$ is the leave-one-out kernel estimator (16) with γ replaced by $\hat{\gamma}^{(d)}$ and based on a bandwidth h . We choose the optimal bandwidth on the interval $[0.1, 0.5]$ based on $h^{(d+1)} = \arg \min_h \text{CV}^{(d+1)}(h)$. For the SMCI-S approach, we utilise the cubic-spline, with the number of knots set to 3, 8, and 10 in Scenarios 1, 2, and 3, respectively.

To evaluate the performance of these three estimators for incidence, the average squared error (ASE) is considered as a criterion, given by $\text{ASE}(\hat{p}) = M^{-1} \sum_{i=1}^M \{\hat{g}(\hat{\gamma}^\top \mathbf{X}_i) - g(\gamma^\top \mathbf{X}_i)\}^2$. It is computed over a grid of points $(\mathbf{x}_j)_j = (\{x_{j1}, x_{j2}, x_{j3},\})_j$, $j = 1, \dots, M$, where M is the number of value sets. For X_1 and X_2 , we use a grid of size 0.1 over $[-1, 2]$ and $[-1.5, 1.5]$ respectively, while X_3 takes values in $\{0, 1\}$, resulting in $M = 1992$. For the latency component, we compute the following metrics of $\hat{\beta}$, over R simulation replicates: the Bias,

$$\text{Bias}(\hat{\beta}) = \frac{1}{R} \sum_{r=1}^R (\hat{\beta}^{(r)} - \beta);$$

the empirical estimated standard error (ESE),

$$\text{ESE}(\hat{\beta}) = \frac{1}{R} \sum_{r=1}^R \widehat{SE}^{(r)};$$

the empirical standard deviation (ESD):

$$\text{ESD}(\hat{\beta}) = \sqrt{\frac{1}{R-1} \sum_{r=1}^R (\hat{\beta}^{(r)} - \bar{\beta})^2}, \text{ where } \bar{\beta} = \frac{1}{R} \sum_{r=1}^R \hat{\beta}^{(r)};$$

and 95% empirical coverage probability (CP), defined as the proportion of replicates in which the nominal 95% confidence interval, $\hat{\beta}^{(r)} \pm 1.96 \times \widehat{SE}(\hat{\beta}^{(r)})$, contains the true parameter β .

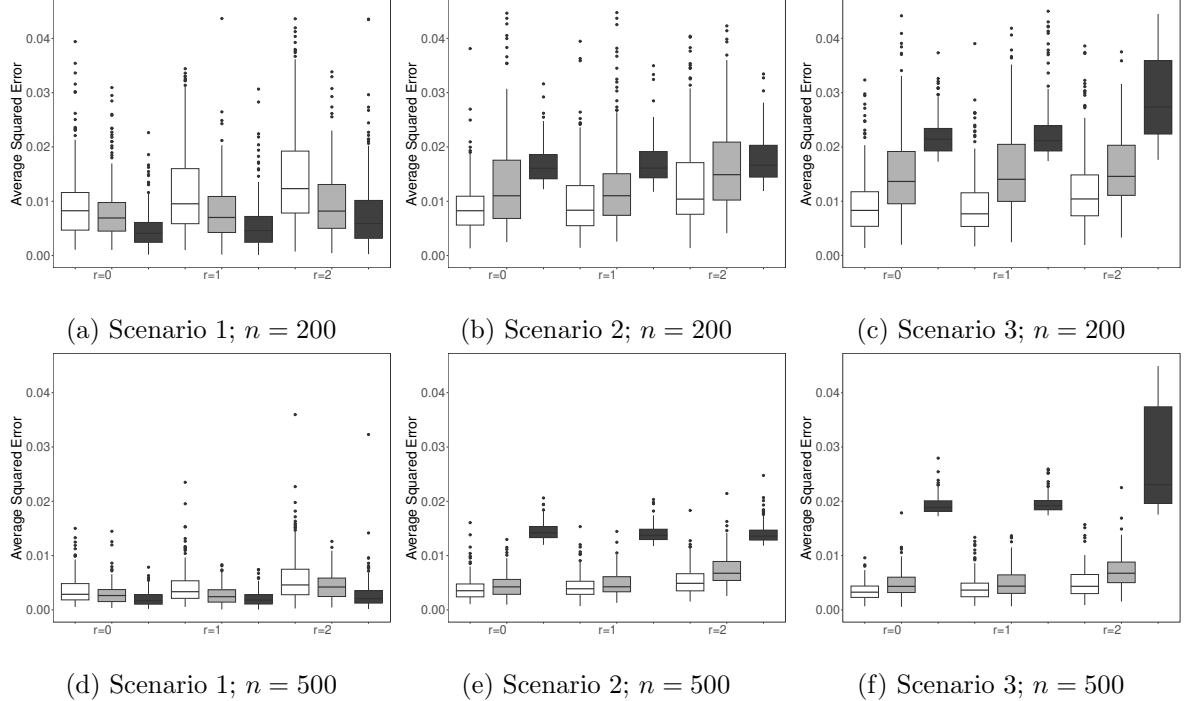


Figure 1: Boxplots of ASE for the SMCI-K (white boxplots), SMCI-S (grey boxplots) and GORMC (dark boxplots) models with $n = 200$ and 500.

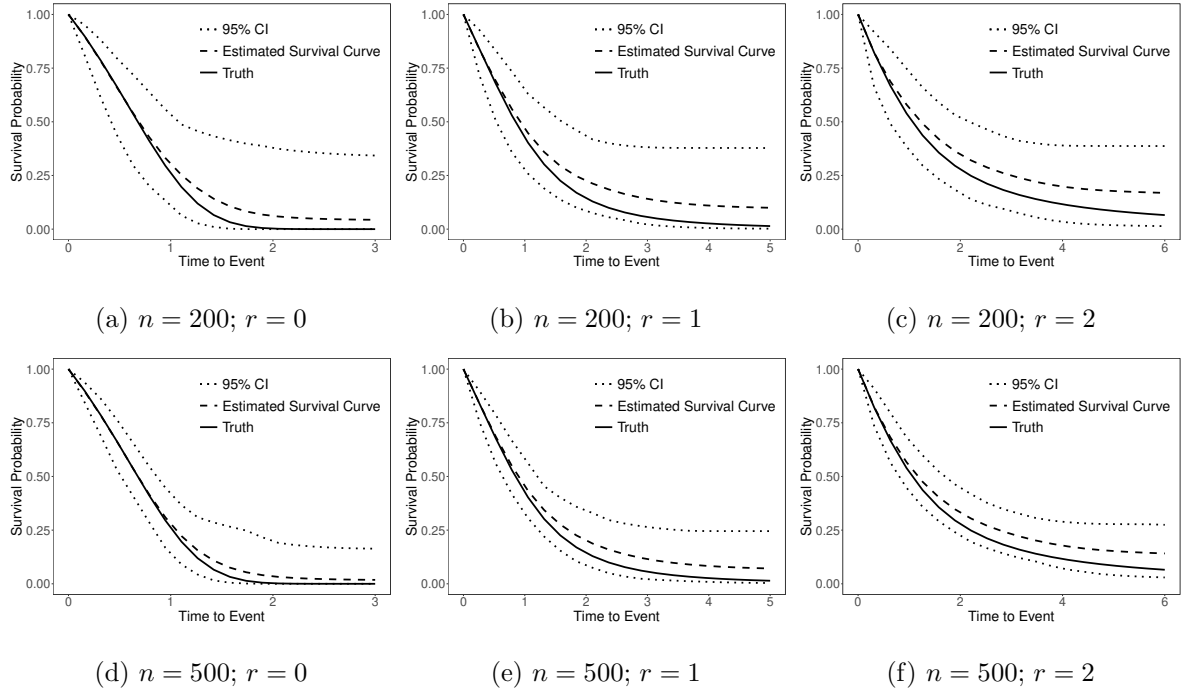


Figure 2: Estimated baseline survival functions $S_u(\cdot | \mathbf{Z} = 0)$ for Scenario 1. The solid curves show the true values, the dashed curves pertain to averaged estimates, and the dotted curves represent the upper and lower 2.5% quantiles of the estimates.

For the incidence, Figure 1 displays the boxplots of the average squared errors (ASEs) of $\hat{p}(\mathbf{X})$ obtained from the proposed SMCI-K, SMCI-S, and the GORMC methods. It shows that the proposed SMCI-K and SMCI-S methods demonstrate outstanding performance compared to the GORMC in some cases. The ASEs for SMCI-K and SMCI-S are generally smaller than those from the GORMC method, regardless of the value of r . An exception occurs in Scenario 1, where the underlying model is correctly specified, and all three methods exhibit small ASEs. The SMCI-K approach achieves lower ASEs than SMCI-S in small-sample settings, with comparable performance at large sample sizes. Both of them produce more outliers compared to the GORMC approach, due to their sensitivity to small changes or noise in the data, especially with small sample sizes. Overall, the results indicate that the proposed methods typically perform well and are preferable to the GORMC method when the true underlying model of the data is unknown.

For the latency component, Tables 1-3 present the summary statistics of $\hat{\beta}$ in three scenarios for the three models. The SMCI-K and SMCI-S approaches yield smaller biases for β relative to the GORMC method except in Scenario 1. A significant advantage is observed in the case

$r = 2$ and $n = 500$, which may arise from the fact that the inaccurate estimate of the **incidence** has a greater impact on the estimate of β when the number of censored observations is large. Figures 2-4 exhibit the estimated baseline survival curves, which slightly deviate from the true curves when $p(\mathbf{X})$ is correctly specified and reveal negligible bias otherwise.

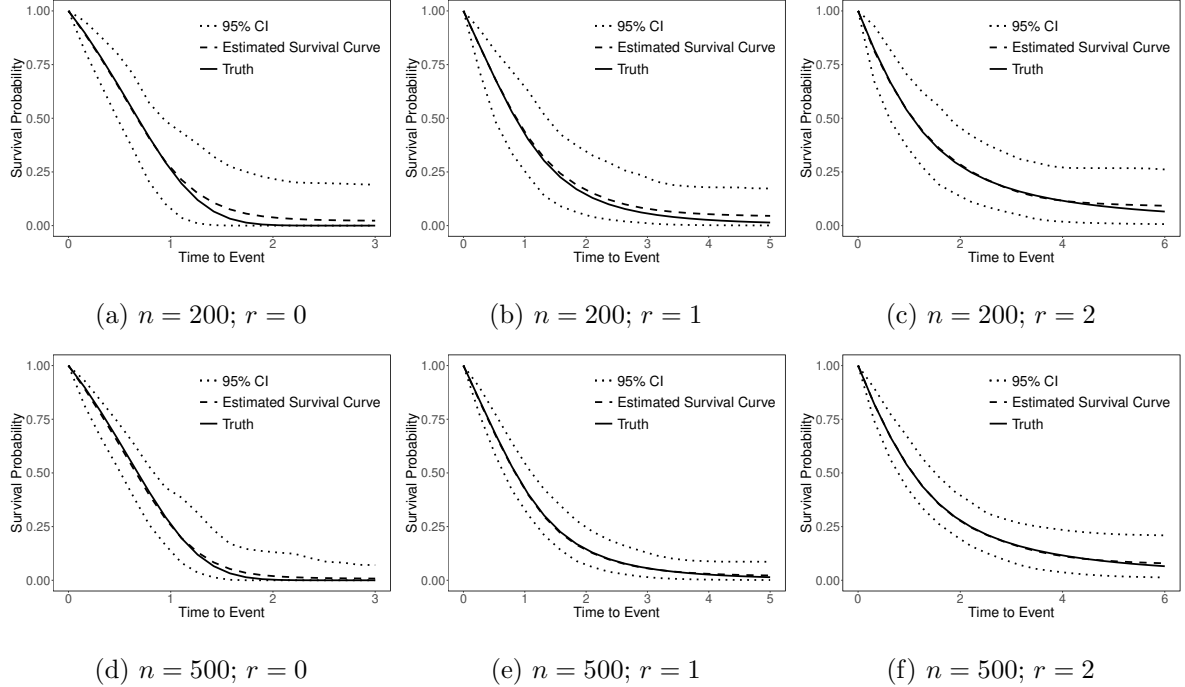


Figure 3: Estimated baseline survival functions $S_u(\cdot | \mathbf{Z} = 0)$ for Scenario 2. The solid curves show the true values, the dashed curves pertain to averaged estimates, and the dotted curves represent the upper and lower 2.5% quantiles of the estimates.

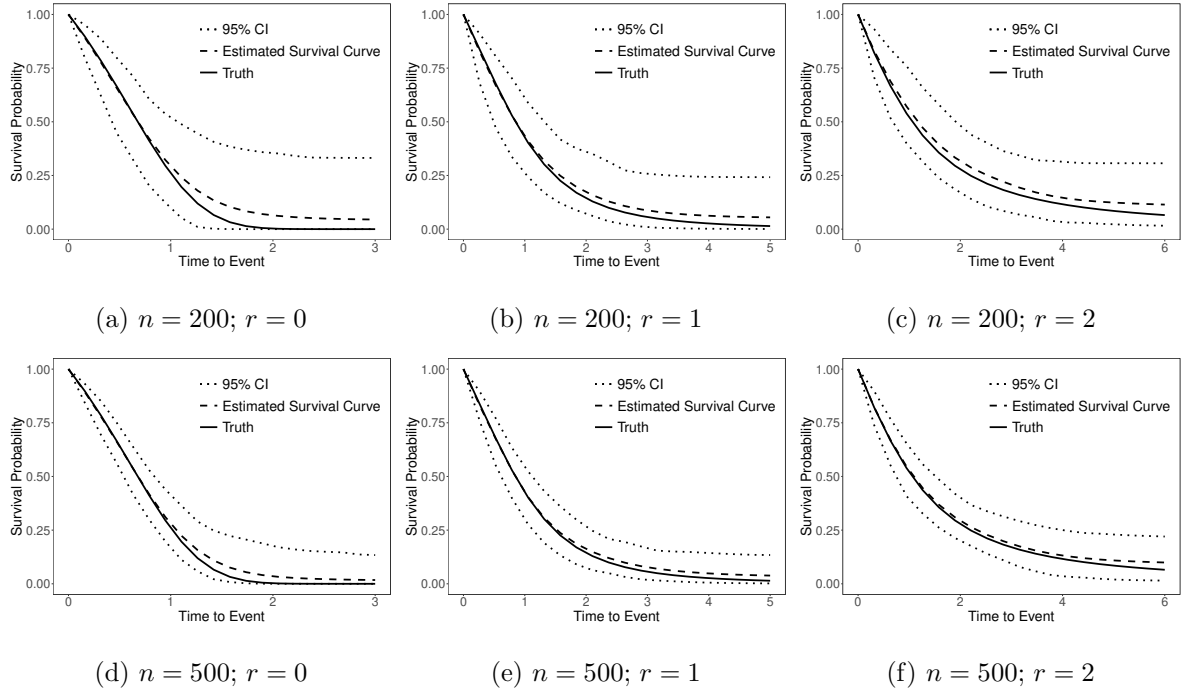


Figure 4: Estimated baseline survival functions $S_u(\cdot | \mathbf{Z} = 0)$ for Scenario 3. The solid curves show the true values, the dashed curves pertain to averaged estimates, and the dotted curves represent the upper and lower 2.5% quantiles of the estimates.

We also examine the performance of the estimated incidence link functions. As expected, the estimated averages closely align with the true values, suggesting that the proposed SMCI-K and SMCI-S models provide accurate approximations (Appendix Figures 8-9).

We perform extensive simulations to further evaluate the method's numerical robustness and computational performance. Robustness checks against varying spline orders and knot specifications confirm stable estimation accuracy (Appendix Tables 6-7 and Figures 10-11). Assessment of scalability with increasing covariate dimensions demonstrates numerical stability and linear time complexity, validating computational efficiency in large dimensional settings (Appendix Table 8 and Figures 12-13). Finally, detailed diagnostics of the EM algorithm, encompassing iteration plots and sensitivity to diverse initial values, verify its reliable convergence (typically within 50–150 iterations) and insensitivity to initialization (Appendix Table 9 and Figures 14-17). All supporting results are provided in Appendix A.4.

Table 1: Simulation result of Scenario 1 with $n = 200$ and 500 . Bias: the estimated bias; ESD: empirical standard deviation; ESE: empirical standard error estimate; CP: the 95% empirical coverage probabilities.

r	Par	SMCI-K				SMCI-S				GORMC			
		Bias	ESD	ESE	CP	Bias	ESD	ESE	CP	Bias	ESD	ESE	CP
$n = 200$													
	β_1	0.02	0.26	0.26	0.94	0.07	0.24	0.25	0.94	0.06	0.24	0.24	0.95
0	β_2	0.00	0.16	0.18	0.98	-0.05	0.18	0.17	0.94	-0.05	0.14	0.17	0.97
	β_3	0.01	0.30	0.30	0.94	0.07	0.32	0.28	0.92	0.06	0.27	0.27	0.96
	β_1	-0.03	0.33	0.34	0.94	0.01	0.34	0.35	0.96	0.00	0.34	0.33	0.93
1	β_2	0.05	0.20	0.21	0.96	-0.02	0.20	0.22	0.94	0.02	0.22	0.21	0.94
	β_3	0.01	0.35	0.39	0.98	0.04	0.37	0.40	0.95	0.04	0.36	0.38	0.97
	β_1	-0.06	0.41	0.41	0.94	0.03	0.41	0.43	0.96	-0.01	0.43	0.41	0.94
2	β_2	0.03	0.22	0.25	0.96	-0.01	0.25	0.27	0.95	-0.02	0.24	0.25	0.96
	β_3	-0.06	0.47	0.48	0.94	-0.02	0.47	0.50	0.96	-0.03	0.48	0.47	0.93
$n = 500$													
	β_1	0.01	0.14	0.16	0.96	0.03	0.16	0.15	0.93	0.02	0.14	0.15	0.94
0	β_2	0.01	0.09	0.11	0.96	-0.01	0.11	0.10	0.94	-0.01	0.09	0.10	0.98
	β_3	-0.01	0.17	0.17	0.95	0.03	0.17	0.16	0.95	0.00	0.16	0.16	0.96
	β_1	0.00	0.20	0.21	0.96	-0.03	0.20	0.21	0.96	0.01	0.21	0.20	0.96
1	β_2	0.03	0.12	0.13	0.96	0.00	0.13	0.13	0.93	0.01	0.12	0.13	0.94
	β_3	-0.01	0.23	0.24	0.92	-0.02	0.24	0.24	0.94	0.00	0.23	0.23	0.92
	β_1	-0.06	0.26	0.25	0.93	-0.03	0.26	0.26	0.96	-0.02	0.26	0.26	0.93
2	β_2	0.05	0.15	0.15	0.94	0.02	0.16	0.16	0.95	0.01	0.16	0.16	0.95
	β_3	-0.03	0.29	0.29	0.95	-0.01	0.29	0.30	0.97	0.00	0.30	0.29	0.95

Table 2: Simulation result of Scenario 2 with $n = 200$ and 500 . Bias: the estimated bias; ESD: empirical standard deviation; ESE: empirical standard error estimate; CP: the 95% empirical coverage probabilities.

r	Par	SMCI-K				SMCI-S				GORMC			
		Bias	ESD	ESE	CP	Bias	ESD	ESE	CP	Bias	ESD	ESE	CP
$n = 200$													
	β_1	0.01	0.22	0.24	0.96	0.03	0.22	0.23	0.96	0.03	0.23	0.24	0.95
0	β_2	-0.01	0.16	0.17	0.94	-0.03	0.16	0.16	0.94	-0.03	0.16	0.16	0.93
	β_3	0.00	0.27	0.27	0.95	0.03	0.26	0.26	0.97	0.03	0.27	0.26	0.92
	β_1	-0.01	0.27	0.32	0.96	0.02	0.33	0.33	0.96	0.01	0.28	0.31	0.98
1	β_2	0.02	0.19	0.19	0.96	-0.01	0.21	0.20	0.94	-0.01	0.20	0.20	0.96
	β_3	0.01	0.34	0.36	0.95	0.06	0.34	0.37	0.96	0.04	0.35	0.36	0.95
	β_1	0.00	0.41	0.40	0.95	0.04	0.43	0.42	0.94	0.04	0.42	0.4	0.94
2	β_2	0.01	0.23	0.24	0.94	-0.02	0.24	0.26	0.95	-0.03	0.24	0.24	0.94
	β_3	0.01	0.46	0.46	0.96	0.00	0.49	0.48	0.94	0.04	0.48	0.45	0.94
$n = 500$													
	β_1	-0.03	0.15	0.15	0.94	0.01	0.14	0.14	0.95	0.00	0.14	0.14	0.96
0	β_2	0.01	0.11	0.11	0.95	0.00	0.10	0.09	0.96	-0.01	0.09	0.09	0.96
	β_3	-0.01	0.17	0.16	0.94	0.02	0.15	0.15	0.94	0.02	0.16	0.15	0.95
	β_1	-0.01	0.18	0.19	0.98	-0.01	0.19	0.20	0.95	0.01	0.19	0.19	0.98
1	β_2	0.00	0.12	0.12	0.96	0.01	0.12	0.12	0.96	-0.02	0.12	0.12	0.96
	β_3	0.01	0.20	0.22	0.96	-0.03	0.23	0.22	0.94	0.02	0.20	0.22	0.96
	β_1	0.00	0.24	0.24	0.96	0.00	0.25	0.25	0.95	0.03	0.25	0.24	0.96
2	β_2	0.00	0.14	0.14	0.96	0.02	0.15	0.16	0.96	-0.03	0.14	0.15	0.97
	β_3	0.01	0.25	0.28	0.97	0.01	0.28	0.29	0.96	0.04	0.27	0.28	0.96

Table 3: Simulation result of Scenario 3 with $n = 200$ and 500 . Bias: the estimated bias; ESD: empirical standard deviation; ESE: empirical standard error estimate; CP: the 95% empirical coverage probabilities.

r	Par	SMCI-K				SMCI-S				GORMC			
		Bias	ESD	ESE	CP	Bias	ESD	ESE	CP	Bias	ESD	ESE	CP
$n = 200$													
	β_1	0.00	0.23	0.25	0.94	0.03	0.24	0.24	0.94	0.05	0.23	0.23	0.95
0	β_2	0.03	0.17	0.17	0.96	-0.03	0.14	0.16	0.98	-0.03	0.16	0.16	0.95
	β_3	-0.04	0.26	0.28	0.96	0.03	0.24	0.26	0.99	0.01	0.25	0.25	0.96
	β_1	-0.03	0.33	0.33	0.94	0.09	0.33	0.34	0.93	-0.02	0.35	0.31	0.92
1	β_2	-0.02	0.19	0.20	0.95	-0.04	0.20	0.21	0.96	-0.02	0.21	0.20	0.92
	β_3	-0.05	0.35	0.37	0.96	0.02	0.38	0.38	0.96	-0.04	0.37	0.35	0.92
	β_1	0.03	0.39	0.40	0.96	0.01	0.44	0.42	0.93	-0.04	0.40	0.36	0.92
2	β_2	0.02	0.23	0.24	0.95	-0.02	0.25	0.26	0.95	0.08	0.27	0.23	0.89
	β_3	0.05	0.47	0.46	0.94	0.03	0.45	0.48	0.96	-0.02	0.46	0.42	0.92
$n = 500$													
	β_1	-0.01	0.14	0.15	0.96	0.00	0.14	0.14	0.98	0.02	0.12	0.14	0.98
0	β_2	0.02	0.10	0.11	0.97	0.01	0.09	0.09	0.97	0.00	0.09	0.09	0.97
	β_3	-0.02	0.18	0.17	0.94	-0.03	0.15	0.16	0.98	0.02	0.16	0.16	0.93
	β_1	-0.01	0.19	0.20	0.98	-0.01	0.20	0.20	0.95	-0.02	0.19	0.19	0.96
1	β_2	0.01	0.12	0.12	0.94	-0.01	0.13	0.13	0.96	0.02	0.13	0.12	0.93
	β_3	-0.03	0.22	0.22	0.95	-0.02	0.23	0.23	0.92	-0.04	0.23	0.22	0.95
	β_1	-0.04	0.24	0.24	0.93	0.00	0.23	0.25	0.96	-0.14	0.26	0.22	0.83
2	β_2	0.02	0.16	0.14	0.92	0.02	0.14	0.16	0.96	0.12	0.18	0.14	0.78
	β_3	0.01	0.26	0.28	0.96	0.02	0.31	0.29	0.93	-0.09	0.26	0.26	0.91

5 Real Data Analysis

As an illustration, we apply our approach to the analysis of the motivating data from the Alzheimer’s Disease Neuroimaging Initiative (ADNI) (Weiner et al., 2015, 2017a,b). MCI, regarded as a transitional stage between normal cognition and more severe AD, is a potential target for identifying individuals at risk of developing AD. The main objective of this study is to identify the risk factors associated with the conversion of time from MCI to the onset of AD in elderly patients. In the dataset, individuals were in states of normal cognitive function, MCI, or AD, with direct transitions from MCI to death being rare; consequently, mortality had a negligible influence as a competing risk in our analysis. Additional information about the dataset can be found on the official website (<https://adni.loni.usc.edu>). The ADNI dataset consists of 950 patients, and 63% of them had never developed severe AD by the end of the study. Figure 5(a) presents the nonparametric maximum likelihood estimator of the survival function. The estimated survival curve plateaus around 0.4, indicating the existence of a proportion of unsusceptible subjects in the population.

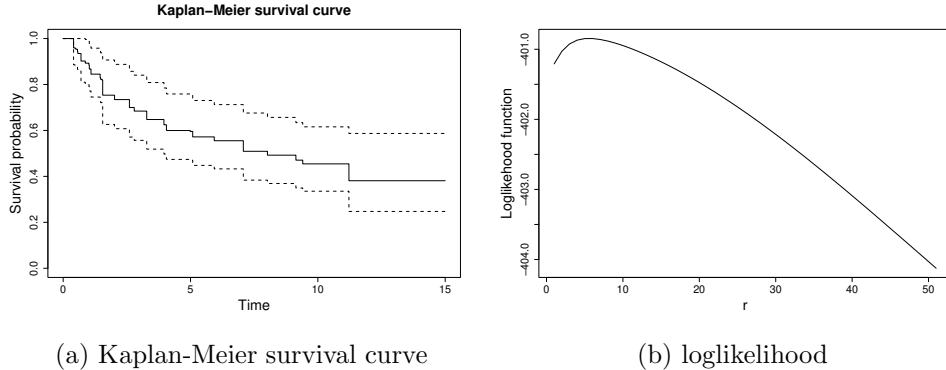


Figure 5: Analysis of the ADNI study: (a) The Kaplan-Meier survival curve; (b) the loglikelihood at the nonparametric maximum likelihood estimates plotted as a function of r in the logarithmic transformations.

In our analysis, we include four baseline prognostic factors in the model for both the latency and incidence components: age (ranged from 55 to 91), gender (0 for female and 1 for male), years of education (ranged from 4 to 20), and APOE4 status (0 for carrying no APOE alleles, 1 for carrying 1 APOE allele and 2 for carrying 2 APOE alleles). We fit model (1) with the class of logarithmic transformations $G(x) = r^{-1} \log(1 + rx)$ ($r \geq 0$). The dataset is partitioned into a training ($n = 633$) and a validation ($n = 317$) sets. The training set is utilised for model

estimation, while the validation set evaluates log-likelihood to select the tuning parameter r for SMCI-K, SMCI-S and GORMC models. The turning parameter r is selected via grid search over the interval $[0,5]$ with a step size of 0.1. As depicted in Figure 5(b), the log-likelihood for the SMCI-K model is maximized at $r = 0.3$, yielding a maximum value of -400.95 . Similarly, for the SMCI-S model, the log-likelihood is maximized at $r = 0$, corresponding to a value of -403.25 . For the GORMC model, the optimal value is $r = 0$, corresponding to a log-likelihood of -410.94 .

Table 4 summarises the estimation results for regression coefficients, standard errors and p-values obtained from these three methods. The larger log-likelihood value and the smaller AIC and BIC values indicate that the SMCI-K performs better than the SMCI-S and GORMC models in predicting survival probability.

Table 4: Analysis Results for ADNI Data under the SMCI and GORMC models.

	SMCI-K			SMCI-S			GORMC		
	Est.	SE	p-value	Est.	SE	p-value	Est.	SE	p-value
Incidence									
(intercept)	-	-	-	-	-	-	-0.09	0.27	0.75
Age	0.59	0.20	0.00*	0.51	0.14	0.00*	0.74	0.16	0.00*
Gender	0.07	0.34	0.83	-0.07	0.26	0.80	0.06	0.29	0.84
Edu	-0.09	0.22	0.67	-0.09	0.13	0.47	-0.04	0.15	0.78
APOE4	0.80	0.33	0.02*	0.85	0.11	0.00*	1.53	0.29	0.00*
Latency									
Age	-0.03	0.17	0.85	-0.06	0.11	0.57	-0.19	0.17	0.28
Gender	-0.30	0.22	0.17	-0.31	0.21	0.14	-0.21	0.32	0.52
Edu	0.08	0.11	0.43	0.09	0.10	0.34	0.03	0.15	0.83
APOE4	0.41	0.19	0.03*	0.28	0.14	0.05*	0.35	0.23	0.13
log-likelihood									
AIC	-400.95			-403.25			-410.94		
BIC	1563.43			1581.96			1570.59		
	1634.64			1653.16			1646.25		

* p-value ≤ 0.05

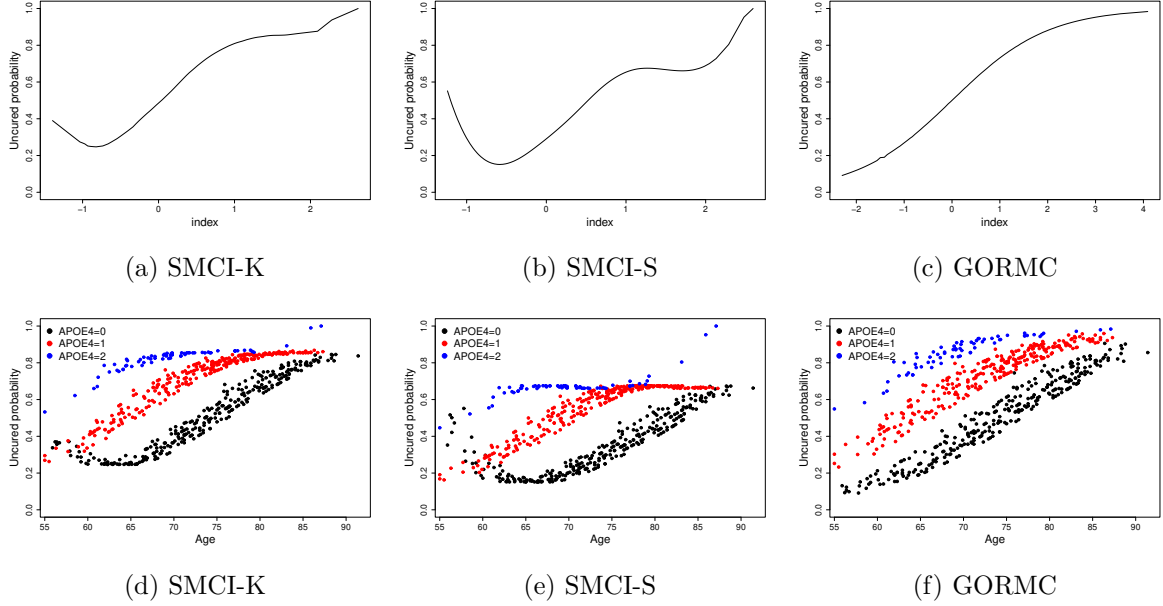


Figure 6: Estimated link functions for (a) the SMCI-K model, (b) the SMCI-S model, (c) the GORMC model, and plots of age effects on the uncure probability for (d) the SMCI-K model, (e) the SMCI-S model and (f) the GORMC model.

For the incidence component, results indicate that both age and APOE4 status have a significant effect (at the 5% level) across all three models. Figures 6(a)-(c) illustrate the estimated link functions. The GORMC model consistently exhibits a clear increasing trend, whereas the SMCI-K and SMCI-S methods reveal a non-monotonic pattern with both decreasing and increasing trends. To exhibit the covariates effects on the uncured probability, Figures 6(d)-(f) present age effects for different APOE4 statuses, as modeled by the three methods. In the GORMC model, the lines representing APOE4 groups do not cross, preserving their relative order. In contrast, the SMCI-K and SMCI-S approaches reveal that the age-related effects on the uncured probability vary across different APOE4 statuses. Specifically, individuals homozygous for APOE4 (carrying two alleles) consistently exhibit the highest uncured probability across all ages, which aligns with evidence that APOE4 homozygosity accelerates amyloid- β accumulation and sustains elevated risk (Safieh et al., 2019; Emrani et al., 2020). For individuals carrying a single APOE4 allele, the uncured probability also demonstrates an increasing trend with age. Among non-carriers, the uncured probability initially decreases with age until approximately 65 years, then subsequently increases. This non-linear effect likely reflects cumulative neurodegenerative and vascular aging processes.

For the latency component, Table 4 indicates that APOE4 status is the only significant predictor of the conditional survival probability among susceptible subjects under the SMCI-K and SMCI-S models. Conversely, no covariates achieve statistical significance in the GORMC model. In the SMCI-K and SMCI-S models, individuals with one or two APOE4 alleles progress from MCI to AD more rapidly than non-carriers, exhibiting a clear dose-response pattern in progression risk. The estimated survival curves from the SMCI-K model (Figure 7) provide consistent visual evidence, showing lower survival probabilities for APOE4 carriers.

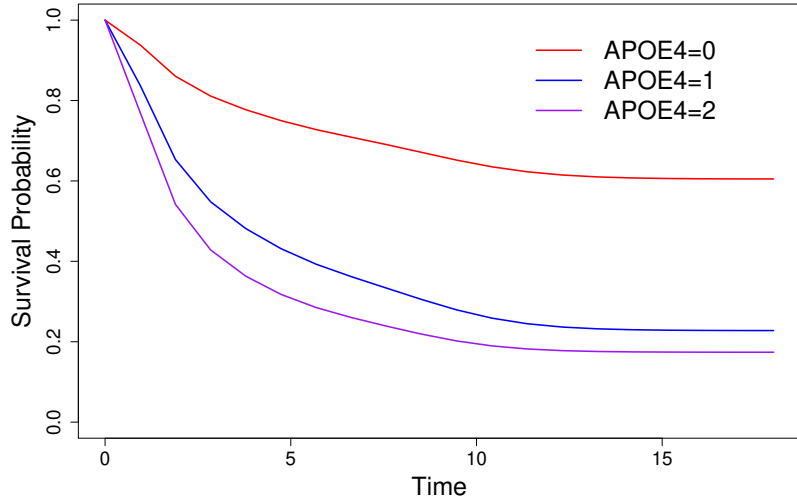


Figure 7: Estimated survival curves in the SMCI-K model for the average level and three different APOE4 status.

6 Conclusion

We proposed a class of flexible single-index semiparametric transformation cure models for analyzing interval-censored data with a cured subgroup, which includes a flexible single-index model for incidence and a semiparametric transformation model for latency. Our proposal allows interpretability and avoids the potential curse-of-dimensionality issue for large dimension covariates in the incidence and includes the proportional hazard cure, proportional odds cure and generalized odds cure models as special cases. We introduce the four-layer data augmentation to facilitate the computation of estimation and obtain the maximum likelihood estimation via the EM algorithm. The numerical study demonstrates that both the SMCI-K and SMCI-S methods provide more accurate estimations than the logistic-based transformation cure method unless

the model is correctly specified, which is robust to the model assumptions. We recommend the utilization of the kernel-based approach in the small-sample setting.

Note that we employed the log-likelihood values, AIC and BIC as the criterion to evaluate model performance. To check the existence of nonlinear effects in the mixture cure model, one can utilize the graphical procedure (Scolas et al., 2018). Recently, Müller and Van Keilegom (2019) proposed tests for the parametric form of the cure rate function with a single covariate. However, the test for the single-index model in the incidence components, which allows for multidimensional covariates, remains to be investigated in the future.

A promising direction for future research is to establish the large-sample properties of the proposed estimator. Although extensive numerical studies provide empirical evidence for the consistency of the estimators, a rigorous formal theoretical proof of consistency and asymptotic normality remains a significant open challenge. Despite recent developments in the theoretical foundation of the single-index model with censored data (Groeneboom and Hendrickx, 2018; Li et al., 2023), the literature on the theoretical properties of single-index mixture cure models remains relatively limited. Musta and Yuen (2024) investigated the consistency of estimators for the single-index mixture cure model with right censored data under monotonicity constraints. A potential direction of research would be on the large-sample properties of estimators for a single-index mixture cure model with interval censoring. Moreover, our proposal assumes the conditional independence of the failure time and the observational process. More complex censoring mechanisms, including informative censoring (Yu et al., 2022; Wang et al., 2016b) and bivariate interval-censored data (Zhou et al., 2017), could be explored. In addition, our method only incorporates nonparametric effects of risk factors on the incidence part while presuming a linear constriction on the latency. The more flexible double semiparametric models should be considered (Lee et al., 2024). These extensions raise theoretical and computational challenges, and further investigation is required.

Acknowledgment

This research was supported by the National Social Science Fund of China (24CTJ035).

Appendix

The Appendix includes the deduction of the complete likelihood function, derivations of the conditional expectations in the expectation-maximization algorithm, the proofs of identifiability, and results from additional simulation studies.

A.1 Deduction of equation (6) to (4) in Section 3.1

We derive the equation (6) to (4) given in section 3.1 of the manuscript. In (6), B_i is the latent cure indicator, Y_{il} s and W_{il} s are independent Poisson random variables conditional on ξ_i with the mean parameters $\lambda_{il}\xi_i$ and $\omega_{il}\xi_i$, respectively, where

$$\lambda_{il} = \eta_l \exp(\boldsymbol{\beta}^\top \mathbf{Z}_i) \{ \delta_{L_i} b_l(R_i) + \delta_{I_i} b_l(L_i) \},$$

$$\omega_{il} = \eta_l \exp(\boldsymbol{\beta}^\top \mathbf{Z}_i) [\delta_{I_i} \{ b_l(R_i) - b_l(L_i) \} + \delta_{R_i} b_l(L_i)].$$

Under the above construction, we can consider $(\mathbf{Y}_l, \mathbf{W}_l, \boldsymbol{\xi}, \mathbf{B})$ as missing data. The complete-data likelihood contributed for the individual $i = 1, \dots, n$ is

$$\begin{aligned} L^{(i)} = & p(\mathbf{X}_i)^{B_i} \{1 - p(\mathbf{X}_i)\}^{1-B_i} f(\xi_i) \prod_{l=1}^k \left\{ \frac{(\lambda_{il}\xi_i)^{Y_{il}}}{Y_{il}!} e^{-\lambda_{il}\xi_i} \right\}^{\delta_{L_i}} \times \left\{ \frac{(\omega_{il}\xi_i)^{W_{il}}}{W_{il}!} e^{-(\omega_{il}+\lambda_{il})\xi_i} \right\}^{\delta_{I_i}} \\ & \times \exp(-\delta_{R_i} B_i \omega_{il} \xi_i) \end{aligned} \quad (19)$$

under the constraint $\delta_{L_i} I(\sum_{l=1}^k Y_{il} > 0) + \delta_{I_i} I(\sum_{l=1}^k W_{il} > 0) + \delta_{R_i} = 1$.

Firstly, for $\delta_{L_i} = 1$, we have $B_i = 1$, $P(B_i = 1) = 1$ and $W_{il} \equiv 0$ since $\omega_{il} = 0$. Equation (19) can be rewritten as $L^{(i)} = p(\mathbf{X}_i) f(\xi_i) \left\{ I(\sum_{l=1}^k Y_{il} > 0) \prod_{l=1}^k \frac{(\lambda_{il}\xi_i)^{Y_{il}}}{Y_{il}!} e^{-\lambda_{il}\xi_i} \right\}$. Integrating Y_{il} , W_{il} , ξ_i and B_i out of $L^{(i)}$, we obtain

$$\begin{aligned} & \int_{\xi_i} \sum_{B_i} \sum_{Y_{il}} \sum_{W_{il}} p(\mathbf{X}_i) f(\xi_i) \left\{ I(\sum_{l=1}^k Y_{il} > 0) \prod_{l=1}^k \frac{(\lambda_{il}\xi_i)^{Y_{il}}}{Y_{il}!} e^{-\lambda_{il}\xi_i} \right\} dW_{il} dY_{il} dB_i d\xi_i \\ & = p(\mathbf{X}_i) \int_{\xi_i} f(\xi_i) \left[1 - \exp\{-\xi_i \exp(\boldsymbol{\beta}^\top \mathbf{Z}_i) \Lambda(R_i)\} \right] d\xi_i. \end{aligned} \quad (20)$$

Similarly, if $\delta_{I_i} = 1$, we have $B_i = 1$ and $P(B_i = 1) = 1$. Equation (19) can be rewritten as $L^{(i)} = p(\mathbf{X}_i) f(\xi_i) \left\{ I(\sum_{l=1}^k Y_{il} = 0, \sum_{l=1}^k W_{il} > 0) \prod_{l=1}^k \frac{(\omega_{il}\xi_i)^{W_{il}}}{W_{il}!} e^{-(\lambda_{il}+\omega_{il})\xi_i} \right\}$. Integrating Y_{il} ,

W_{il} , ξ_i and B_i out of $L^{(i)}$, we have

$$\begin{aligned} & \int_{\xi_i} \sum_{B_i} \sum_{Y_{il}} \sum_{W_{il}} p(\mathbf{X}_i) f(\xi_i) \left\{ I\left(\sum_{l=1}^k Y_{il} = 0, \sum_{l=1}^k W_{il} > 0\right) \frac{(\omega_i \xi_i)^{(W_{il})}}{W_{il}!} e^{-(\lambda_{il} + \omega_{il}) \xi_i} \right\} dW_{il} dY_{il} dB_i d\xi_i \\ &= p(\mathbf{X}_i) \int_{\xi_i} f(\xi_i) \left[\exp\{-\xi_i \exp(\boldsymbol{\beta}^\top \mathbf{Z}_i) \Lambda(L_i)\} - \exp\{-\xi_i \exp(\boldsymbol{\beta}^\top \mathbf{Z}_i) \Lambda(R_i)\} \right] d\xi_i. \end{aligned} \quad (21)$$

Finally, if $\delta_{R_i} = 1$, we have $Y_{il} \equiv 0$ since $\lambda_{il} = 0$. Equation (19) can be rewritten as $L^{(i)} = p(\mathbf{X}_i)^{B_i} \{1 - p(\mathbf{X}_i)\}^{1-B_i} f(\xi_i) \exp\{-I(\sum_{l=1}^k Y_{il} = 0, \sum_{l=1}^k W_{il} = 0) B_i \omega_i \xi_i\}$. Note that $P(B_i = 1) = p(\mathbf{X}_i)$ is defined at the beginning of Section 3.1. Integrating Y_{il} , W_{il} , ξ_i and B_i out of $L^{(i)}$, it follows that

$$\begin{aligned} & \int_{\xi_i} \sum_{B_i} \sum_{Y_{il}} \sum_{W_{il}} p(\mathbf{X}_i)^{B_i} \{1 - p(\mathbf{X}_i)\}^{1-B_i} f(\xi_i) \prod_{l=1}^k \exp\{-I(\sum_{l=1}^k W_{il} = 0) B_i \omega_{il} \xi_i\} dW_{il} dY_{il} dB_i d\xi_i \\ &= \int_{\xi_i} f(\xi_i) \left[1 - p(\mathbf{X}_i) + p(\mathbf{X}_i) \exp\{-\xi_i \exp(\boldsymbol{\beta}^\top \mathbf{Z}_i) \Lambda(L_i)\} \right] d\xi_i. \end{aligned} \quad (22)$$

Combining (20), (21) and (22) gives

$$\begin{aligned} & \int_{\xi} \sum_{B_i} \sum_{Y_{il}} \sum_{W_{il}} L_4(\boldsymbol{\theta} | \mathcal{O}, \mathbf{B}, \boldsymbol{\xi}, \mathbf{Y}, \mathbf{W}) dW_{il} dY_{il} dB_i d\xi \\ &= \prod_{i=1}^n p(\mathbf{X}_i)^{1-\delta_{R_i}} \int_{\xi_i} \left[1 - \exp\{-\xi_i \exp(\boldsymbol{\beta}^\top \mathbf{Z}_i) \Lambda(R_i)\} \right]^{\delta_{R_i}} \\ & \quad \times \left[\exp\{-\xi_i \exp(\boldsymbol{\beta}^\top \mathbf{Z}_i) \Lambda(L_i)\} - \exp\{-\xi_i \exp(\boldsymbol{\beta}^\top \mathbf{Z}_i) \Lambda(R_i)\} \right]^{\delta_{I_i}} \\ & \quad \times \left[1 - p(\mathbf{X}_i) + p(\mathbf{X}_i) \exp\{-\xi_i \exp(\boldsymbol{\beta}^\top \mathbf{Z}_i) \Lambda(L_i)\} \right]^{\delta_{R_i}} f(\xi_i) d\xi_i \\ &= L(\boldsymbol{\theta} | \mathcal{O}_o). \end{aligned}$$

Therefore, (4) can be derived by integrating out \mathbf{Y}_l s, \mathbf{W}_l s $\boldsymbol{\xi}$ and \mathbf{B} in (6).

A.2 Proof of Conditional expectations

We derive the expressions for expectations given in Section 3.3 of the manuscript. As discussed in Section 3.1, Y_i and W_i conditionally follow the truncated Poisson distribution with the mean

parameter $\lambda_i^{(d)}\xi_i$ and $\omega_i^{(d)}\xi_i$, respectively, where

$$\begin{aligned}\lambda_i^{(d)} &= \exp(\boldsymbol{\beta}^{(d)\top} \mathbf{Z}_i) \{ \delta_{L_i} \sum_{l=1}^k \eta_l^{(d)} b_l(R_i) + \delta_{I_i} \sum_{l=1}^k \eta_l^{(d)} b_l(L_i) \} \\ \omega_i^{(d)} &= \exp(\boldsymbol{\beta}^{(d)\top} \mathbf{Z}_i) \delta_{I_i} [\{ \sum_{l=1}^k \eta_l^{(d)} b_l(R_i) - \sum_{l=1}^k \eta_l^{(d)} b_l(L_i) \} + \delta_{R_i} \sum_{l=1}^k \eta_l^{(d)} b_l(L_i)].\end{aligned}$$

The posterior density function of ξ_i given the observed data is proportional to $p(\mathbf{X}_i) \{1 - S_u(R_i|\mathbf{Z}_i)\}^{\delta_{L_i}} \{S_u(L_i|\mathbf{Z}_i) - S_u(R_i|\mathbf{Z}_i)\}^{\delta_{I_i}} S_u(L_i|\mathbf{Z}_i)^{\delta_{R_i}}$, where

$$S_u(T_i|\mathbf{Z}_i) = \exp\{-\xi_i \exp(\boldsymbol{\beta}^{(d)\top} \mathbf{Z}_i) \sum_{l=1}^k \eta_l^{(d)} b_l(T_i)\}.$$

We first consider $E(Y_i|\boldsymbol{\theta}^{(d)}, \mathcal{O})$. For $i = 1, \dots, n$, we have

$$\begin{aligned}E(Y_i|\boldsymbol{\theta}^{(d)}, \mathcal{O}) &= E(Y_i|\boldsymbol{\theta}^{(d)}, \mathcal{O}, Y_i > 0) P(Y_i > 0|\boldsymbol{\theta}^{(d)}, \mathcal{O}) \\ &= E(E(Y_i|\xi_i, \boldsymbol{\theta}^{(d)}, \mathcal{O}, Y_i > 0)|\boldsymbol{\theta}^{(d)}, \mathcal{O}, Y_i > 0) P(Y_i > 0|\boldsymbol{\theta}^{(d)}, \mathcal{O}),\end{aligned}$$

where the outer expectation above is taken with respect to the distribution of ξ_i given $\boldsymbol{\theta}^{(d)}, \mathcal{O}$ and $Y_i > 0$. It follows that

$$E(Y_i|\xi_i, \boldsymbol{\theta}^{(d)}, \mathcal{O}, Y_i > 0) = \begin{cases} \frac{\xi_i N_{i2}^{(d)}}{1 - \exp(-\xi_i N_{i2}^{(d)})}, & \text{if } \delta_{L_i} = 1, \\ 0, & \text{if } \delta_{I_i} = 1 \text{ or } \delta_{R_i} = 1, \end{cases} \quad (23)$$

where $N_{i2}^{(d)} = \exp(\boldsymbol{\beta}^{(d)\top} \mathbf{Z}_i) \sum_{l=1}^k \eta_l^{(d)} b_l(R_i)$. This can be rewritten as

$$E(Y_i|\xi_i, \boldsymbol{\theta}^{(d)}, \mathcal{O}, Y_i > 0) = \frac{\delta_{L_i} \xi_i N_{i2}^{(d)}}{1 - \exp(-\xi_i N_{i2}^{(d)})},$$

and hence

$$E(Y_i|\boldsymbol{\theta}^{(d)}, \mathcal{O}, Y_i > 0) = \frac{\delta_{L_i} N_{i2}^{(d)} \int_{\xi_i} \xi_i f(\xi_i) d\xi_i}{1 - \exp\{-G(N_{i2}^{(d)})\}}. \quad (24)$$

Similarly, for $E(W_i|\boldsymbol{\theta}^{(d)}, \mathcal{O})$, we have

$$\begin{aligned} E(W_i|\boldsymbol{\theta}^{(d)}, \mathcal{O}) &= E(W_i|\boldsymbol{\theta}^{(d)}, \mathcal{O}, W_i > 0)P(W_i > 0|\boldsymbol{\theta}^{(d)}, \mathcal{O}) \\ &= E(E(W_i|\xi_i, \boldsymbol{\theta}^{(d)}, \mathcal{O}, W_i > 0)|\boldsymbol{\theta}^{(d)}, \mathcal{O}, W_i > 0)P(W_i > 0|\boldsymbol{\theta}^{(d)}, \mathcal{O}), \end{aligned}$$

where the outer expectation above is taken with respect to the distribution of ξ_i given $\boldsymbol{\theta}^{(d)}, \mathcal{O}$ and $W_i > 0$. It follows that

$$E(W_i|\xi_i, \boldsymbol{\theta}^{(d)}, \mathcal{O}, W_i > 0) = \begin{cases} \frac{\xi_i(N_{i2}^{(d)} - N_{i1}^{(d)})}{1 - \exp\{-\xi_i(N_{i2}^{(d)} - N_{i1}^{(d)})\}}, & \text{if } \delta_{I_i} = 1, \\ 0, & \text{if } \delta_{L_i} = 1 \text{ or } \delta_{R_i} = 1, \end{cases}$$

where $N_{i1}^{(d)} = \exp(\boldsymbol{\beta}^{(d)\top} \mathbf{Z}_i) \sum_{l=1}^k \eta_l^{(d)} b_l(L_i)$. This can be rewritten as

$$E(W_i|\xi_i, \boldsymbol{\theta}^{(d)}, \mathcal{O}, W_i > 0) = \frac{\delta_{I_i} \xi_i (N_{i2}^{(d)} - N_{i1}^{(d)})}{1 - \exp\{-\xi_i(N_{i2}^{(d)} - N_{i1}^{(d)})\}},$$

and hence

$$E(W_i|\boldsymbol{\theta}^{(d)}, \mathcal{O}) = \frac{\delta_{I_i} (N_{i2}^{(d)} - N_{i1}^{(d)}) \exp\{-G(N_{i1}^{(d)})\} G'(N_{i1}^{(d)})}{\exp\{-G(N_{i1}^{(d)})\} - \exp\{-G(N_{i2}^{(d)})\}}. \quad (25)$$

Then we drive the expectations for $E(Y_{il}|\boldsymbol{\theta}^{(d)}, \mathcal{O})$ and $(W_{il}|\boldsymbol{\theta}^{(d)}, \mathcal{O})$. Noting that the distribution of Y_{il} given Y_i and the distribution of W_{il} given W_i are both binomial. Thus,

$$E(Y_{il}|\boldsymbol{\theta}^{(d)}, \mathcal{O}) = \frac{\eta_l^{(d)} b_l(R_i) E(Y_i|\boldsymbol{\theta}^{(d)}, \mathcal{O})}{\sum_{l=1}^k \eta_l^{(d)} b_l(R_i)}, \quad (26)$$

$$E(W_{il}|\boldsymbol{\theta}^{(d)}, \mathcal{O}) = \frac{\eta_l^{(d)} \{b_l(R_i) - b_l(L_i)\} E(W_i|\boldsymbol{\theta}^{(d)}, \mathcal{O})}{\sum_{l=1}^k \eta_l^{(d)} \{b_l(R_i) - b_l(L_i)\}}. \quad (27)$$

We now drive $E(B_i|\boldsymbol{\theta}^{(d)}, \mathcal{O})$. The conditional expectation of B_i is the probability of being cured for the right-censored subject, which is equal to 1 when the failure time is left-censored or interval-censored. Consequently,

$$E(B_i|\boldsymbol{\theta}^{(d)}, \mathcal{O}) = \delta_{L_i} + \delta_{I_i} + \frac{\delta_{R_i} p^{(d)}(X_i) \exp\{-G(N_{i1}^{(d)})\}}{1 - p^{(d)}(X_i) + p^{(d)}(X_i) \exp\{-G(N_{i1}^{(d)})\}}. \quad (28)$$

For $E(\xi_i B_i|\boldsymbol{\theta}^{(d)}, \mathcal{O})$, we have $E(\xi_i B_i|\boldsymbol{\theta}^{(d)}, \mathcal{O}) = E(\xi_i B_i|\boldsymbol{\theta}^{(d)}, \mathcal{O}, B_i = 1)P(B_i = 1|\boldsymbol{\theta}^{(d)}, \mathcal{O})$. For

left-censored subject, $P(\mathcal{O}) = P(B_i = 1, \boldsymbol{\theta}^{(d)}, \mathcal{O}) = p^{(d)}(X_i)(1 - \exp\{-G(N_{i2}^{(d)})\})$, then

$$\begin{aligned} E(\xi_i B_i | \boldsymbol{\theta}^{(d)}, \mathcal{O}) &= \frac{\int_{\xi_i} \xi_i p^{(d)}(X_i) \{1 - \exp(-\xi_i N_{i2}^{(d)})\} f(\xi_i) d\xi_i}{P(\mathcal{O})} \\ &= \frac{\int_{\xi_i} \xi_i f(\xi_i) d\xi_i - \exp\{-G(N_{i2}^{(d)})\} G'(N_{i2}^{(d)})}{1 - \exp\{-G(N_{i2}^{(d)})\}}. \end{aligned}$$

Similarly, for interval-censored subject, $P(\mathcal{O}) = P(B_i = 1, \boldsymbol{\theta}^{(d)}, \mathcal{O}) = p^{(d)}(X_i)[\exp\{-G(N_{i1}^{(d)})\} - \exp\{-G(N_{i2}^{(d)})\}]$. Consequently,

$$\begin{aligned} E(\xi_i B_i | \boldsymbol{\theta}^{(d)}, \mathcal{O}) &= \frac{\int_{\xi_i} \xi_i p^{(d)}(X_i) \{\exp(-\xi_i N_{i1}^{(d)}) - \exp(-\xi_i N_{i2}^{(d)})\} f(\xi_i) d\xi_i}{P(\mathcal{O})} \\ &= \frac{\exp\{-G(N_{i1}^{(d)})\} G'(N_{i1}^{(d)}) - \exp\{-G(N_{i2}^{(d)})\} G'(N_{i2}^{(d)})}{\exp\{-G(N_{i1}^{(d)})\} - \exp\{-G(N_{i2}^{(d)})\}}. \end{aligned}$$

We now consider right-censored subject. If $\delta_{R_i} = 1$, then $P(\mathcal{O}) = 1 - p^{(d)}(X_i) + p^{(d)}(X_i) \exp\{-G(N_{i1}^{(d)})\}$ and $P(\mathcal{O}) = P(B_i = 1, \boldsymbol{\theta}^{(d)}, \mathcal{O}) = p^{(d)}(X_i) \exp\{-G(N_{i1}^{(d)})\}$. It follows that

$$\begin{aligned} E(\xi_i B_i | \boldsymbol{\theta}^{(d)}, \mathcal{O}) &= \frac{\int_{\xi_i} \xi_i p^{(d)}(X_i) \exp(-\xi_i N_{i1}^{(d)}) f(\xi_i) d\xi_i}{P(\mathcal{O})} \\ &= \frac{p^{(d)}(X_i) \exp\{-G(N_{i1}^{(d)})\} G'(N_{i1}^{(d)})}{1 - p^{(d)}(X_i) + p^{(d)}(X_i) \exp\{-G(N_{i1}^{(d)})\}}. \end{aligned}$$

Combining these results gives

$$\begin{aligned} E(\xi_i B_i | \boldsymbol{\theta}^{(d)}) &= \delta_{L_i} \frac{\int_{\xi_i} \xi_i f(\xi_i) d\xi_i - \exp\{-G(N_{i2}^{(d)})\} G'(N_{i2}^{(d)})}{1 - \exp\{-G(N_{i2}^{(d)})\}} \\ &+ \delta_{I_i} \frac{\exp\{-G(N_{i1}^{(d)})\} G'(N_{i1}^{(d)}) - \exp\{-G(N_{i2}^{(d)})\} G'(N_{i2}^{(d)})}{\exp\{-G(N_{i1}^{(d)})\} - \exp\{-G(N_{i2}^{(d)})\}} \\ &+ \delta_{R_i} \frac{p^{(d)}(X_i) \exp\{-G(N_{i1}^{(d)})\} G'(N_{i1}^{(d)})}{1 - p^{(d)}(X_i) + p^{(d)}(X_i) \exp\{-G(N_{i1}^{(d)})\}}. \end{aligned} \tag{29}$$

From Equations (24), (25), (26), (27), (28) and (29), the conditional expectation in Section

3.3 are

$$\begin{aligned}
E(Y_{il}) &= \frac{\eta_l^{(d)} b_l(R_i) E(Y_i)}{\sum_{l=1}^k \eta_l^{(d)} b_l(R_i)}, \quad E(Y_i) = \frac{\delta_{L_i} N_{i2}^{(d)} \int_{\xi_i} \xi_i f(\xi_i) d\xi_i}{1 - \exp\{-G(N_{i2}^{(d)})\}}, \\
E(W_{il}) &= \frac{\eta_l^{(d)} \{b_l(R_i) - b_l(L_i)\} E(W_i)}{\sum_{l=1}^k \eta_l^{(d)} \{b_l(R_i) - b_l(L_i)\}}, \\
E(W_i) &= \frac{\delta_{I_i} (N_{i2}^{(d)} - N_{i1}^{(d)}) \exp\{-G(N_{i1}^{(d)})\} G'(N_{i1}^{(d)})}{\exp\{-G(N_{i1}^{(d)})\} - \exp\{-G(N_{i2}^{(d)})\}}, \\
E(B_i) &= \delta_{L_i} + \delta_{I_i} + \frac{\delta_{R_i} p^{(d)}(\mathbf{X}_i) \exp\{-G(N_{i1}^{(d)})\}}{1 - p^{(d)}(\mathbf{X}_i) + p^{(d)}(\mathbf{X}_i) \exp\{-G(N_{i1}^{(d)})\}},
\end{aligned}$$

and

$$\begin{aligned}
E(\xi_i B_i) &= \delta_{L_i} \frac{\int_{\xi_i} \xi_i f(\xi_i) d\xi_i - \exp\{-G(N_{i2}^{(d)})\} G'(N_{i2}^{(d)})}{1 - \exp\{-G(N_{i2}^{(d)})\}} \\
&\quad + \delta_{I_i} \frac{\exp\{-G(N_{i1}^{(d)})\} G'(N_{i1}^{(d)}) - \exp\{-G(N_{i2}^{(d)})\} G'(N_{i2}^{(d)})}{\exp\{-G(N_{i1}^{(d)})\} - \exp\{-G(N_{i2}^{(d)})\}} \\
&\quad + \delta_{R_i} \frac{p^{(d)}(\mathbf{X}_i) \exp\{-G(N_{i1}^{(d)})\} G'(N_{i1}^{(d)})}{1 - p^{(d)}(\mathbf{X}_i) + p^{(d)}(\mathbf{X}_i) \exp\{-G(N_{i1}^{(d)})\}}.
\end{aligned}$$

A.3 Proof of identifiability

To establish model identifiability, suppose that there exist two parameter sets $(g, \boldsymbol{\gamma}, \Lambda, \boldsymbol{\beta})$ and $(\tilde{g}, \tilde{\boldsymbol{\gamma}}, \tilde{\Lambda}, \tilde{\boldsymbol{\beta}})$ such that for all (\mathbf{X}, \mathbf{Z}) and $t \in [0, \infty)$,

$$1 - g(\boldsymbol{\gamma}^\top \mathbf{X}) + g(\boldsymbol{\gamma}^\top \mathbf{X}) S_u(t|\mathbf{Z}) = 1 - \tilde{g}(\tilde{\boldsymbol{\gamma}}^\top \mathbf{X}) + \tilde{g}(\tilde{\boldsymbol{\gamma}}^\top \mathbf{X}) \tilde{S}_u(t|\mathbf{Z}), \quad (30)$$

where $S_u(t|\mathbf{Z}) = \exp[-G\{\exp(\boldsymbol{\beta}^\top \mathbf{Z})\Lambda(t)\}]$, and $\tilde{S}_u(t|\mathbf{Z}) = \exp[-G\{\exp(\tilde{\boldsymbol{\beta}}^\top \mathbf{Z})\tilde{\Lambda}(t)\}]$. We demonstrate identifiability by showing $g = \tilde{g}$, $\boldsymbol{\gamma} = \tilde{\boldsymbol{\gamma}}$, $\Lambda = \tilde{\Lambda}$, $\boldsymbol{\beta} = \tilde{\boldsymbol{\beta}}$.

From equation (30), we obtain

$$\frac{g(\boldsymbol{\gamma}^\top \mathbf{X})}{\tilde{g}(\tilde{\boldsymbol{\gamma}}^\top \mathbf{X})} = \frac{1 - \tilde{S}_u(t|\mathbf{Z})}{1 - S_u(t|\mathbf{Z})} = c(\mathbf{X}),$$

where $c(\mathbf{X})$ is a positive function of \mathbf{X} independent of t . Rearranging yields $\tilde{S}_u(t|\mathbf{Z}) =$

$c(\mathbf{X})S_u(t|\mathbf{Z}) + 1 - c(\mathbf{X})$. By assumption A(6), $\lim_{t \rightarrow \infty} S_u(t|\mathbf{Z}) = \lim_{t \rightarrow \infty} \tilde{S}_u(t|\mathbf{Z}) = 0$. Hence $c(\mathbf{X}) = 1$, implying $g(\boldsymbol{\gamma}^\top \mathbf{X}) = \tilde{g}(\tilde{\boldsymbol{\gamma}})$ and $S_u(t|\mathbf{Z}) = \tilde{S}_u(t|\mathbf{Z})$.

From the equality of survival functions and the assumption that G is strictly increasing, we have

$$\exp(\boldsymbol{\beta}^\top \mathbf{Z})\Lambda(t) = \exp(\tilde{\boldsymbol{\beta}}^\top \mathbf{Z})\tilde{\Lambda}(t).$$

Rewriting this relationship yields $\frac{\exp(\boldsymbol{\beta}^\top \mathbf{Z})}{\exp(\tilde{\boldsymbol{\beta}}^\top \mathbf{Z})} = \frac{\tilde{\Lambda}(t)}{\Lambda(t)} = c_1$, where c_1 is a positive constant independent of \mathbf{Z} and t . Based on assumption (A4), we have $\boldsymbol{\beta} = \tilde{\boldsymbol{\beta}}$, and $c_1 = 1$, which further implies $\Lambda(t) = \tilde{\Lambda}(t)$.

For the equality $g(\boldsymbol{\gamma}^\top \mathbf{X}) = \tilde{g}(\tilde{\boldsymbol{\gamma}}^\top \mathbf{X})$, the identifiability of parameters can be established based on Theorem 2.1 in Horowitz (2009).

A.4 More simulation results

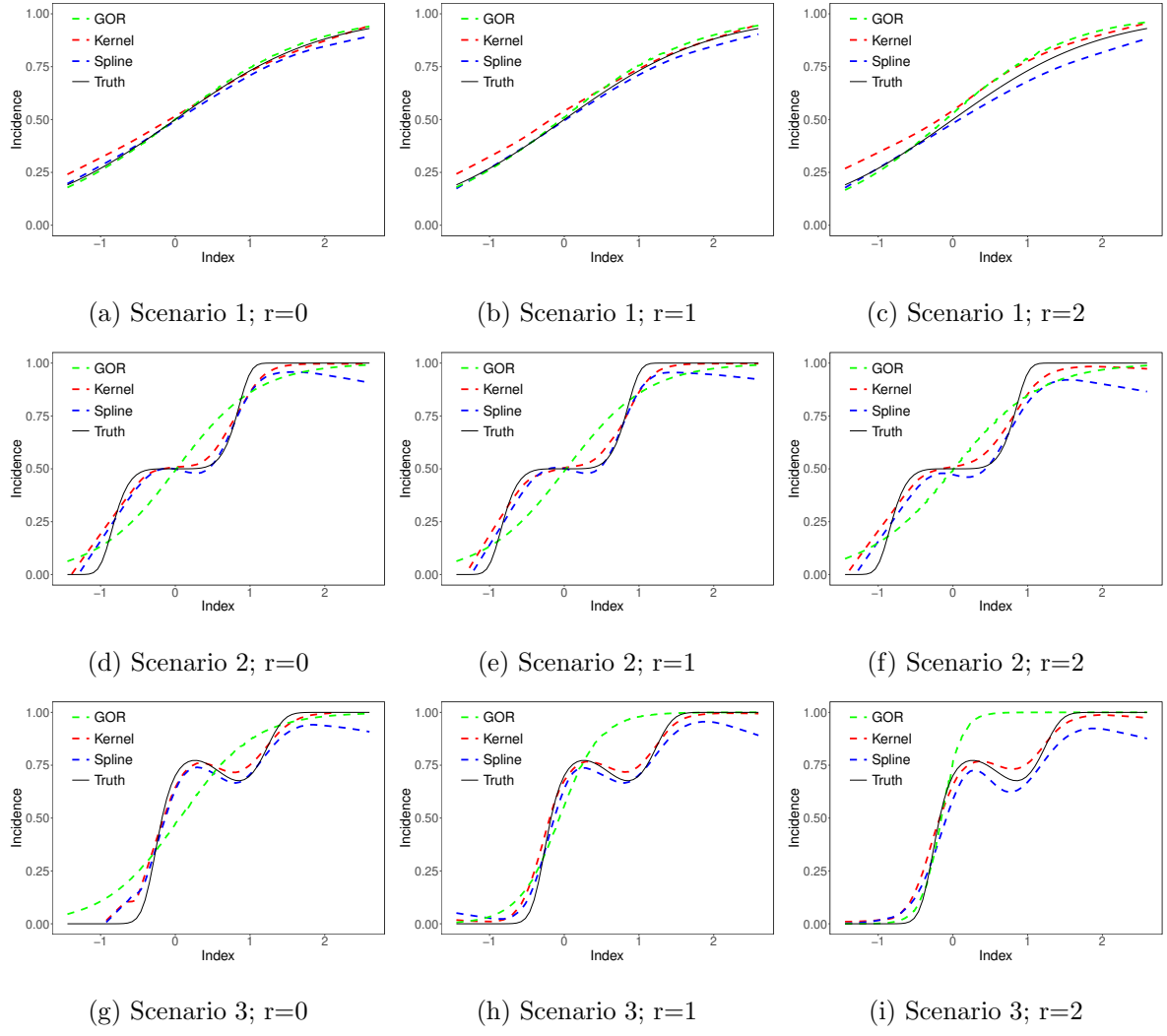


Figure 8: Estimated incidence link functions($n = 200$). True values are shown in black, with method-specific estimates displayed as: kernel method (red), spline regression (blue), and logistic modeling (green).

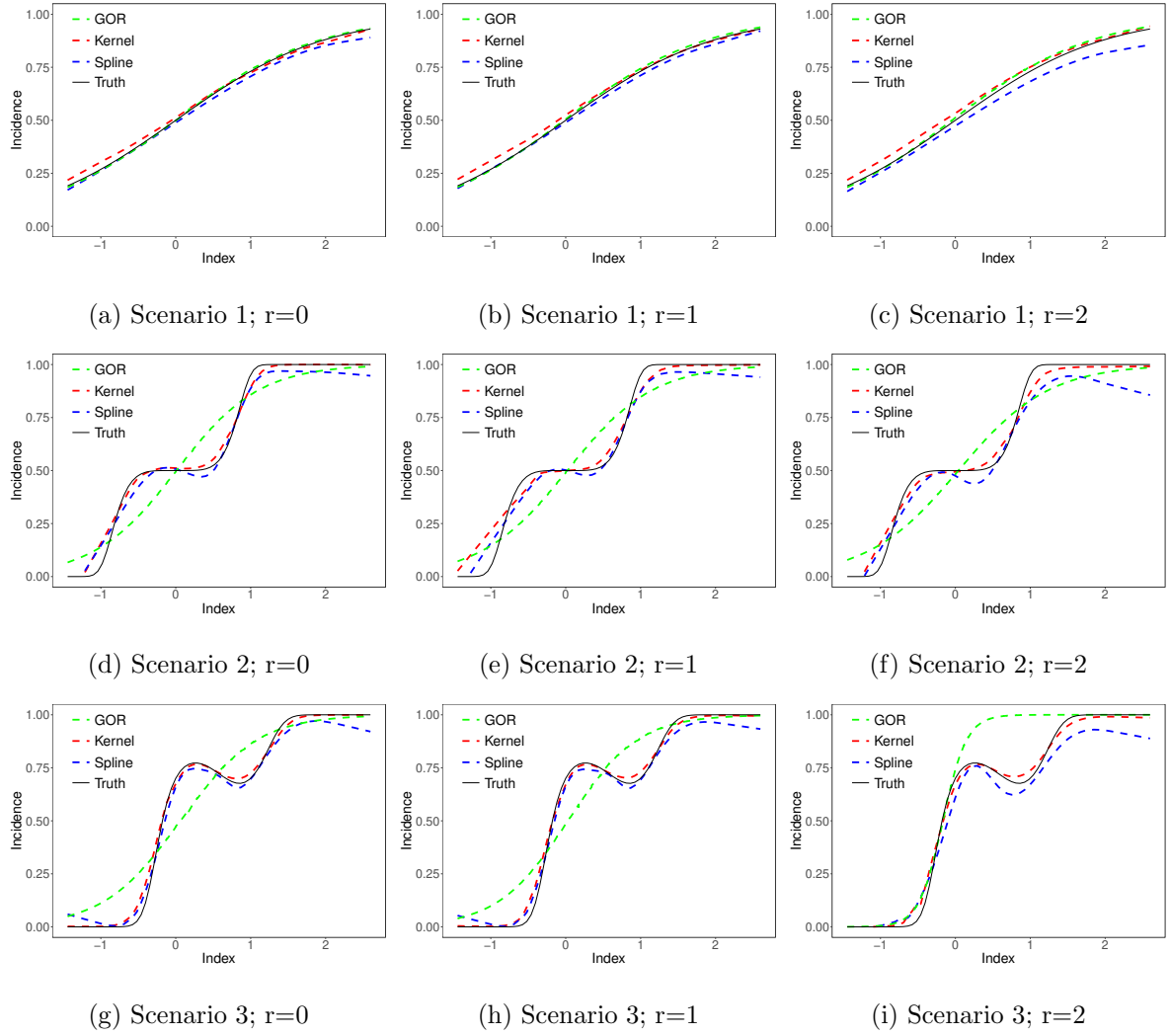


Figure 9: Estimated incidence link functions($n = 500$). True values are shown in black, with method-specific estimates displayed as: kernel method (red), spline regression (blue), and logistic modeling (green).

Table 5: Simulation setting

Scenario	r	κ	ζ	$n = 200$			$n = 500$		
				p_{cure}	p_L	p_R	p_{cure}	p_L	p_R
1	0	3	5	0.38	0.13	0.45	0.38	0.12	0.46
	1	5	5	0.38	0.13	0.44	0.38	0.13	0.45
	2	6	8	0.38	0.12	0.46	0.38	0.12	0.46
2	0	3	5	0.33	0.14	0.41	0.32	0.14	0.41
	1	5	8	0.33	0.14	0.39	0.33	0.14	0.39
	2	6	8	0.32	0.13	0.42	0.32	0.13	0.42
3	0	3	5	0.33	0.13	0.42	0.34	0.13	0.42
	1	5	5	0.33	0.14	0.40	0.34	0.14	0.46
	2	6	8	0.33	0.12	0.42	0.34	0.13	0.45

A.4.1 Sensitivity Analysis: Spline Orders and Knots

To evaluate the impact of spline order and knot specification on model performance, we have conducted additional simulations under Scenario 3 with 200 sample sizes and $r = 1$, varying the spline order (quadratic, cubic, or quartic) and the number of knots (6–8 quantile-based). The results, summarized in Tables 6–7 and Figures 10–11, demonstrate that the estimation performance for both parametric and nonparametric components remains stable and accurate across all tested specifications.

$n = 200$	True	Bias	SSD	SE	CP
Order 2 (quadratic)					
β_1	1	0.00	0.32	0.34	0.95
β_2	-1	0.01	0.20	0.21	0.96
β_3	1	0.01	0.33	0.38	0.98
Order 3 (cubic)					
β_1	1	0.01	0.33	0.34	0.94
β_2	-1	0.00	0.21	0.21	0.96
β_3	1	0.01	0.33	0.38	0.98
Order 4 (quartic)					
β_1	1	0.01	0.33	0.33	0.94
β_2	-1	-0.01	0.21	0.21	0.94
β_3	1	0.02	0.33	0.38	0.97

Table 6: Simulation results for Scenario 3 with $n = 200$ and $r = 1$ using quadratic, cubic, or quartic I-splines. Bias: the estimated bias; ESD: empirical standard deviation; ESE: empirical standard error estimate; CP: the 95% empirical coverage probabilities.

$n = 200$	True	Bias	SSD	SE	CP
6 quantile-based knots					
β_1	1	0.08	0.30	0.33	0.96
β_2	-1	0.00	0.21	0.21	0.93
β_3	1	0.00	0.36	0.38	0.97
7 quantile-based knots					
β_1	1	0.08	0.30	0.33	0.96
β_2	-1	-0.01	0.21	0.21	0.93
β_3	1	0.00	0.36	0.38	0.96
8 quantile-based knots					
β_1	1	0.06	0.32	0.33	0.96
β_2	-1	0.01	0.24	0.38	0.95
β_3	1	-0.01	0.38	0.38	0.95

Table 7: Simulation results of Scenario 3 with $n = 200$ and $r = 1$ using 6-8 quantile-based knots. Bias: the estimated bias; ESD: empirical standard deviation; ESE: empirical standard error estimate; CP: the 95% empirical coverage probabilities.

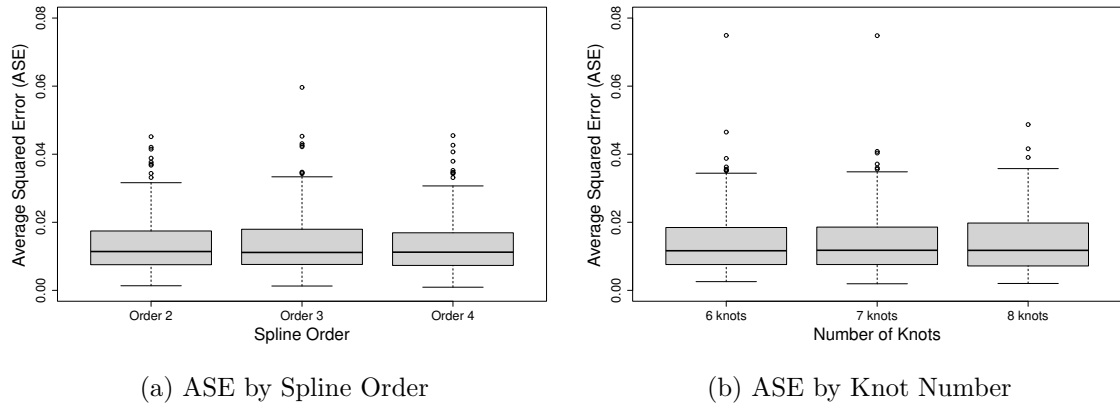


Figure 10: Boxplots of ASE for the incidence link function in Scenario 3 with $n = 200$ and $r = 1$, employing quadratic, cubic, or quartic I-splines (left panel) and 6-8 quantile-based knots (right panel).

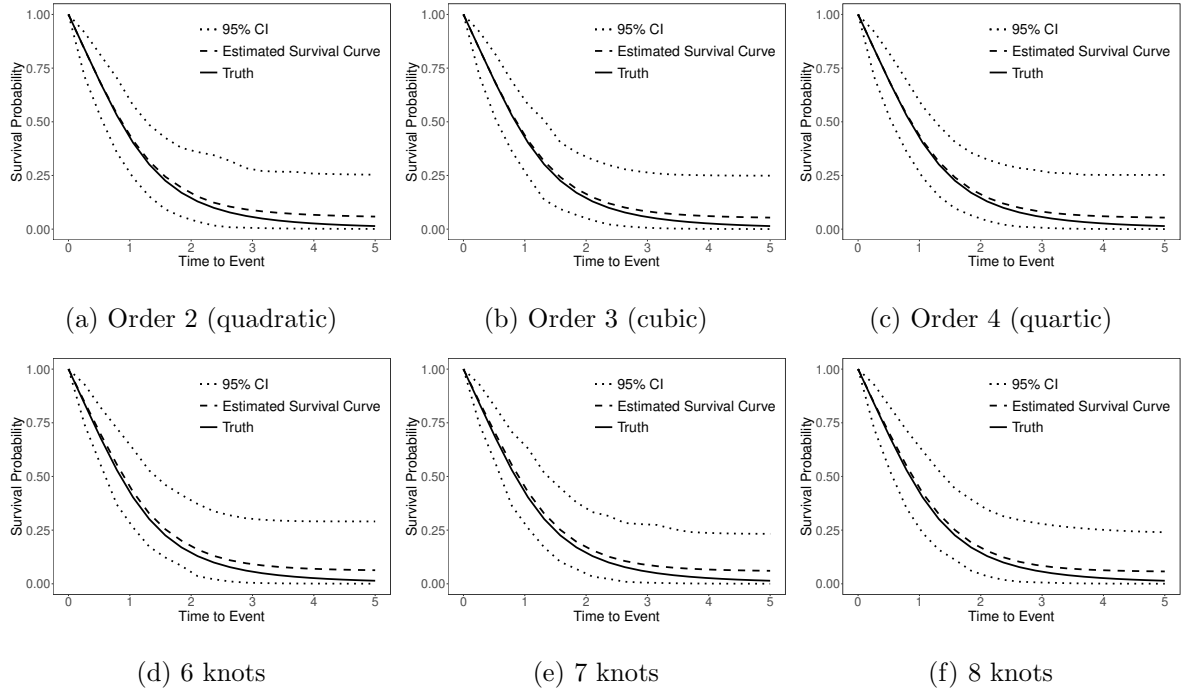


Figure 11: Estimated baseline survival functions of Scenario 3 with $n = 200$ and $r = 1$, employing quadratic, cubic, or quartic I-splines (upper panel) and 6-8 quantile-based knots (lower panel).

A.4.2 Computational Efficiency and Scalability

To empirically assess scalability, we conducted additional simulations with varying covariate dimensions for the incidence (d_1) and latency (d_2) components: $(d_1, d_2) = (5, 5), (10, 10)$. As summarized in Table 8 and Figures 12-13, the results indicate that 1) the running time increases approximately linearly with the total number of covariates. This suggests that the EM algorithm remains efficient for moderate-dimensional settings; and 2) the estimation performance for both parametric and nonparametric components remains stable across dimensions, demonstrating numerical robustness.

(n, d_1, d_2)	Average Time(second)	Avg. Bias	MSE
SMCI-K			
(200,5,5)	64.44	0.01	0.57
(200,10,10)	88.18	-0.04	0.53
SMCI-S			
(200,5,5)	14.20	0.01	0.56
(200,10,10)	23.60	-0.04	0.52

Table 8: Computational time and estimation accuracy under varying covariate dimension d_1 (incidence) and d_2 (latency).

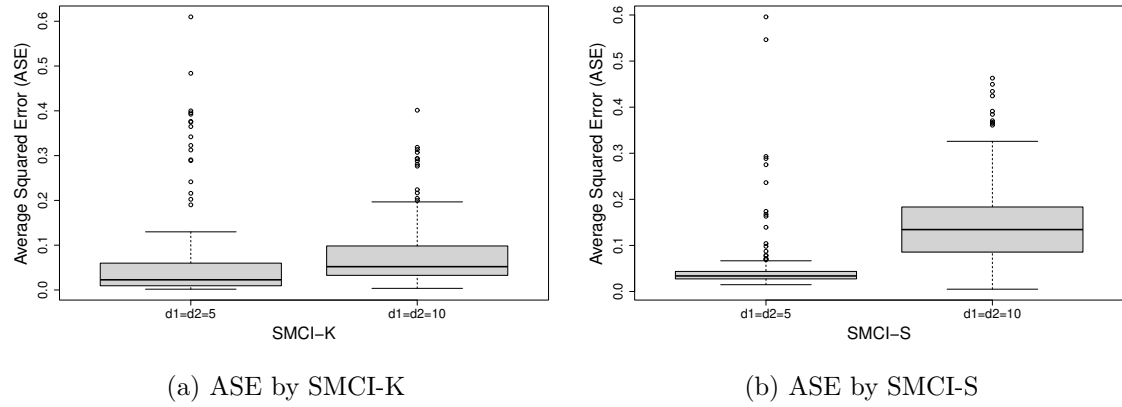


Figure 12: Boxplots of ASE for the incidence link function in Scenario 3 with $n = 500$ and $r = 1$ under varying covariate dimension d_1 (incidence) and d_2 (latency).

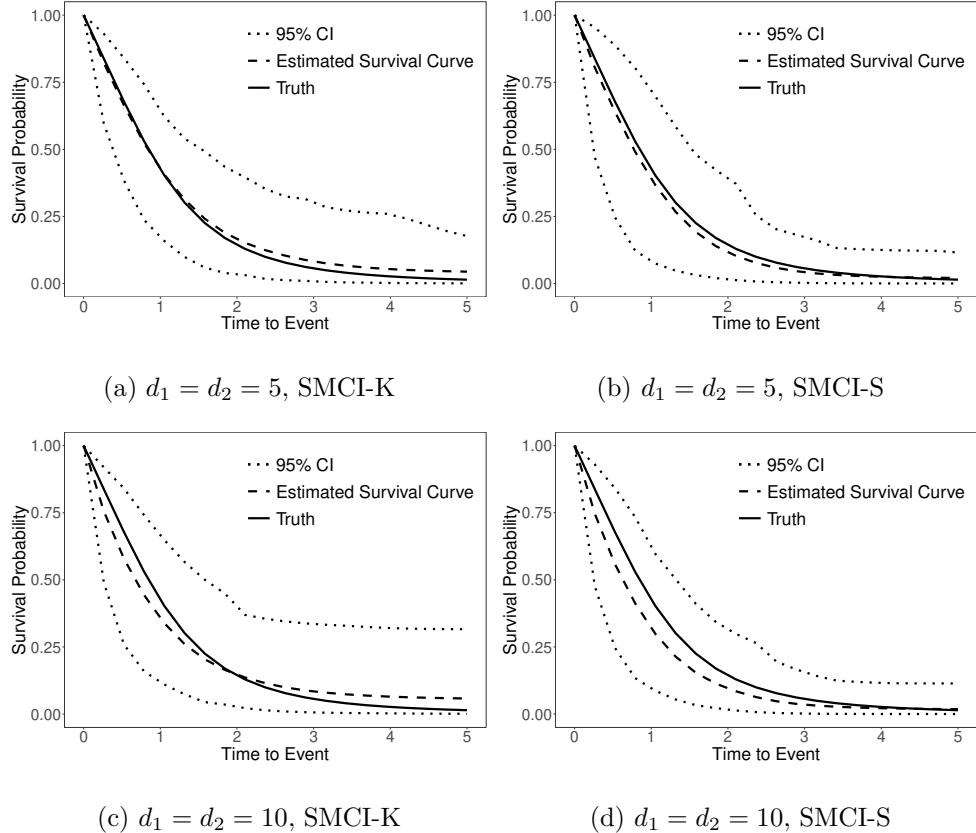


Figure 13: Estimated baseline survival functions of Scenario 3 with $n = 500$ and $r = 1$, under varying covariate dimension d_1 (incidence) and d_2 (latency).

A.4.3 EM Algorithm Diagnostics

For convergence diagnostics, we provide iteration plots showing the evolution of the log-likelihood across EM iterations for proposed models (SMCI-K and SMCI-S). As demonstrated in Figures 14-15, the EM algorithm consistently converged within a reasonable range, typically requiring around 50-150 iterations.

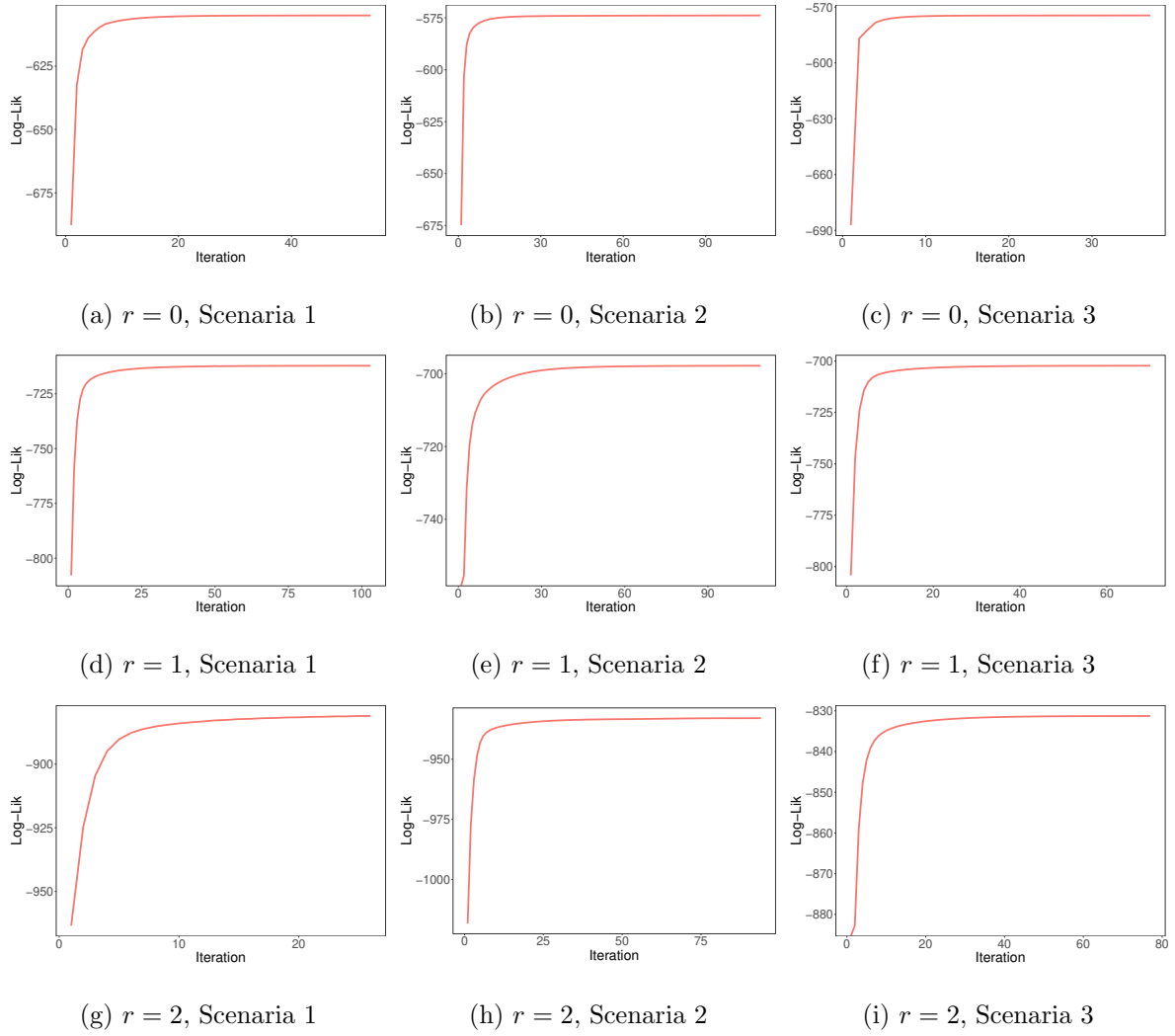


Figure 14: Convergence behavior of the log-likelihood function during SMCI-K algorithm iterations. The first row ($r = 0$), second row ($r = 1$), and third row ($r = 2$) demonstrate how the parameter influences convergence rate and stability in Scenarios 1, 2, and 3 (columns from left to right).

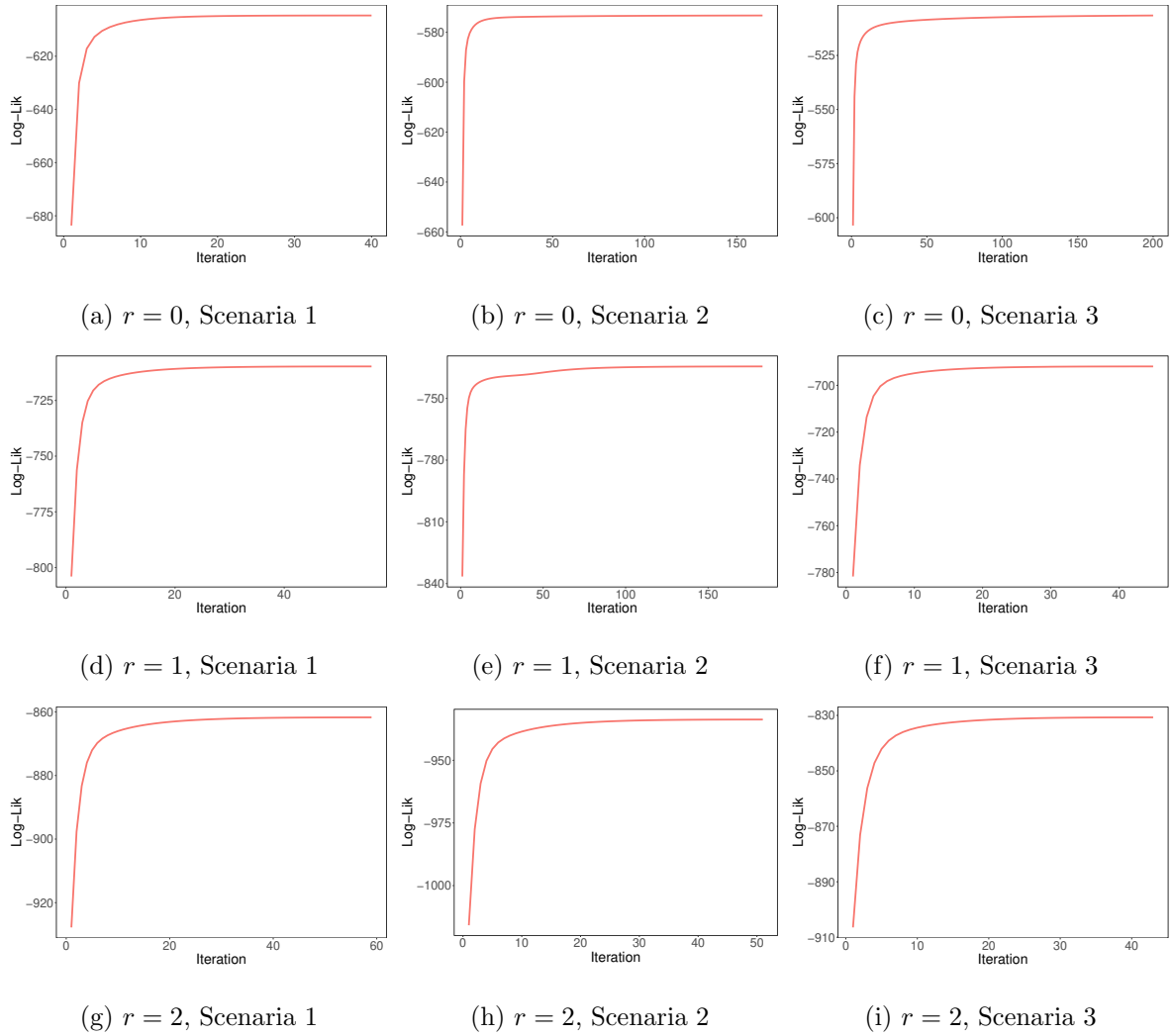


Figure 15: Convergence behavior of the log-likelihood function during SMCI-S algorithm iterations. The first row ($r = 0$), second row ($r = 1$), and third row ($r = 2$) demonstrate how the parameter influences convergence rate and stability in Scenarios 1, 2, and 3 (columns from left to right).

Furthermore, to assess sensitivity to initial values, we performed additional simulation studies with three distinct sets of initial values for β and η :

- Set A : $\beta^{(0)} = (-0.5, -0.5, -0.5)$, $\eta^{(0)} = (0.5, 0.5, \dots, 0.5)$
- Set B: $\beta^{(0)} = (0.5, 0.5, 0.5)$, $\eta^{(0)} = (1.5, 1.5, \dots, 1.5)$
- Set C: $\beta^{(0)} = (-0.5, -0.5, -0.5)$ $\eta^{(0)} = (1.5, 1.5, \dots, 1.5)$

Note $\gamma^{(0)}$ is obtained by fitting the generalized additive model using pseudo values $1 - \delta_{R_i}$, thus we don't consider different initial values for $\gamma^{(0)}$. As summarized in Table 9 and Figures

16-17, the resulting parameter estimates are highly consistent and exhibit negligible bias and proper coverage probabilities across all initializations. This consistency strongly suggests that our algorithm is insensitive to initial values.

$n = 500$	True	Bias	SSD	SE	CP
Set A					
β_1	1	0.03	0.18	0.20	0.96
β_2	-1	-0.02	0.12	0.13	0.96
β_3	1	0.02	0.24	0.23	0.96
Set B					
β_1	1	0.01	0.19	0.20	0.97
β_2	-1	-0.01	0.13	0.13	0.92
β_3	1	0.05	0.22	0.23	0.96
Set C					
β_1	1	-0.02	0.20	0.20	0.94
β_2	-1	-0.02	0.11	0.13	0.96
β_3	1	0.01	0.22	0.23	0.96

Table 9: Simulation results for Scenario 3 with $n = 500$ and $r = 1$ using three sets of initial values. Bias: the estimated bias; ESD: empirical standard deviation; ESE: empirical standard error estimate; CP: the 95% empirical coverage probabilities.

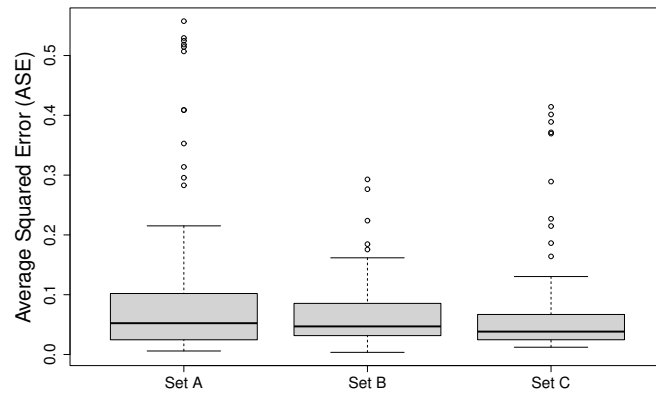


Figure 16: Boxplots of ASE for the incidence link function in Scenario 3 with $n = 500$ and $r = 1$, using three sets of initial values.

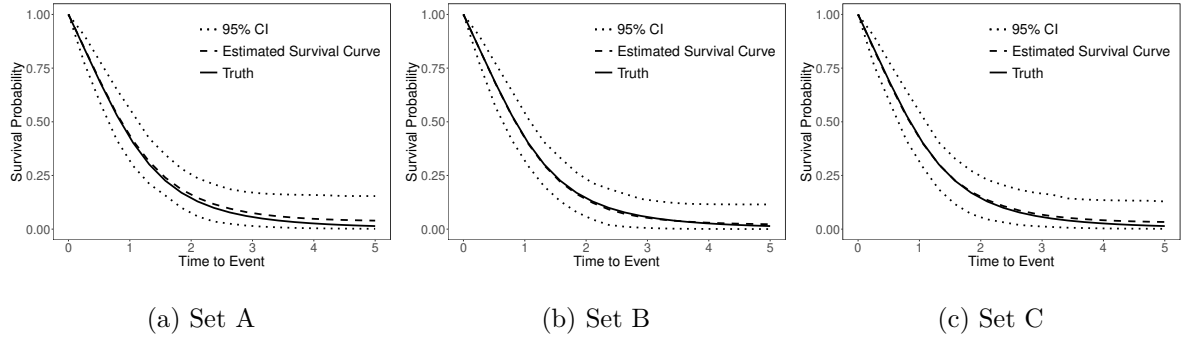


Figure 17: Estimated baseline survival functions of Scenario 3 with $n = 500$ and $r = 1$, using three sets of initial values.

References

Amico, M., Van Keilegom, I., and Legrand, C. (2019). The single-index/cox mixture cure model. *Biometrics*, 75(2):452–462.

Aselisewine, W. and Pal, S. (2023). On the integration of decision trees with mixture cure model. *Statistics in Medicine*, 42(23):4111–4127.

Boag, J. W. (1949). Maximum likelihood estimates of the proportion of patients cured by cancer therapy. *Journal of the Royal Statistical Society. Series B (Methodological)*, 11(1):15–53.

Chen, C. M., Shen, P.-S., and Huang, W. L. (2019). Semiparametric transformation models for interval-censored data in the presence of a cure fraction. *Biometrical Journal*, 61(1):203–215.

Chen, K., Jin, Z., and Ying, Z. (2002). Semiparametric analysis of transformation models with censored data. *Biometrika*, 89(3):659–668.

Ding, Y. and Nan, B. (2011). A sieve m-theorem for bundled parameters in semiparametric models, with application to the efficient estimation in a linear model for censored data. *Annals of statistics*, 39(6):2795.

Emrani, S., Arain, H. A., DeMarshall, C., and Nuriel, T. (2020). Apoe4 is associated with cognitive and pathological heterogeneity in patients with alzheimer’s disease: a systematic review. *Alzheimer’s research & therapy*, 12(1):141.

Fang, H.-B., Li, G., and Sun, J. (2005). Maximum likelihood estimation in a semiparametric logistic/proportional-hazards mixture model. *Scandinavian Journal of Statistics*, 32(1):59–75.

Gorst-Rasmussen, A. and Scheike, T. (2013). Independent screening for single-index hazard rate models with ultrahigh dimensional features. *Journal of the Royal Statistical Society Series B: Statistical Methodology*, 75(2):217–245.

Groeneboom, P. and Hendrickx, K. (2018). Current status linear regression. *The Annals of Statistics*, 46(4):1415–1444.

Horowitz, J. L. (2009). *Semiparametric and Nonparametric Methods in Econometrics*, volume 12. Springer, New York.

Jin, Z., Lin, D., Wei, L., and Ying, Z. (2003). Rank-based inference for the accelerated failure time model. *Biometrika*, 90(2):341–353.

Kim, Y.-J. and Jhun, M. (2008). Cure rate model with interval censored data. *Statistics in medicine*, 27(1):3–14.

Kuk, A. Y. and Chen, C.-H. (1992). A mixture model combining logistic regression with proportional hazards regression. *Biometrika*, 79(3):531–541.

Lam, K., Fong, D. Y., and Tang, O. (2005). Estimating the proportion of cured patients in a censored sample. *Statistics in medicine*, 24(12):1865–1879.

Lam, K. and Xue, H. (2005). A semiparametric regression cure model with current status data. *Biometrika*, 92(3):573–586.

Lee, C. Y., Wong, K. Y., and Bandyopadhyay, D. (2024). Partly linear single-index cure models with a nonparametric incidence link function. *Statistical Methods in Medical Research*, 33(3):498–514.

Li, S., Tian, S., Yu, Y., Zhu, X., and Lian, H. (2023). Corporate probability of default: A single-index hazard model approach. *Journal of Business & Economic Statistics*, 41(4):1288–1299.

Liu, X. and Xiang, L. (2021). Generalized accelerated hazards mixture cure models with interval-censored data. *Computational Statistics & Data Analysis*, 161:107248.

López-Cheda, A., Cao, R., Jácome, M. A., and Van Keilegom, I. (2017). Nonparametric incidence estimation and bootstrap bandwidth selection in mixture cure models. *Computational Statistics & Data Analysis*, 105:144–165.

Lu, W. and Ying, Z. (2004). On semiparametric transformation cure models. *Biometrika*, 91(2):331–343.

Lu, X., Chen, G., Singh, R. S., and K. Song, P. X. (2006). A class of partially linear single-index survival models. *Canadian Journal of Statistics*, 34(1):97–112.

Ma, S. (2009). Cure model with current status data. *Statistica Sinica*, pages 233–249.

Ma, S. (2010). Mixed case interval censored data with a cured subgroup. *Statistica Sinica*, pages 1165–1181.

Mao, M. and Wang, J.-L. (2010). Semiparametric efficient estimation for a class of generalized proportional odds cure models. *Journal of the American Statistical Association*, 105(489):302–311.

Müller, U. U. and Van Keilegom, I. (2019). Goodness-of-fit tests for the cure rate in a mixture cure model. *Biometrika*, 106(1):211–227.

Murphy, S. A. and Van der Vaart, A. W. (2000). On profile likelihood. *Journal of the American Statistical Association*, 95(450):449–465.

Musta, E. and Yuen, T. P. (2024). Single-index mixture cure model under monotonicity constraints. *Electronic Journal of Statistics*, 18(2):3376–3436.

Oulhaj, A., Wilcock, G. K., Smith, A. D., and De Jager, C. A. (2009). Predicting the time of conversion to mci in the elderly: role of verbal expression and learning. *Neurology*, 73(18):1436–1442.

Peng, Y. and Dear, K. B. (2000). A nonparametric mixture model for cure rate estimation. *Biometrics*, 56(1):237–243.

Ramsay, J. O. (1988). Monotone regression splines in action. *Statistical science*, pages 425–441.

Safieh, M., Korczyn, A. D., and Michaelson, D. M. (2019). Apoe4: an emerging therapeutic target for alzheimer's disease. *BMC medicine*, 17(1):64.

Scolas, S., El Ghouch, A., Legrand, C., and Oulhaj, A. (2016). Variable selection in a flexible parametric mixture cure model with interval-censored data. *Statistics in Medicine*, 35(7):1210–1225.

Scolas, S., Legrand, C., Oulhaj, A., and El Ghouch, A. (2018). Diagnostic checks in mixture cure models with interval-censoring. *Statistical Methods in Medical Research*, 27(7):2114–2131.

Sun, J. (2006). *The statistical analysis of interval-censored failure time data*. Springer.

Sun, J., Kopciuk, K. A., and Lu, X. (2008). Polynomial spline estimation of partially linear single-index proportional hazards regression models. *Computational statistics & data analysis*, 53(1):176–188.

Sy, J. P. and Taylor, J. M. (2000). Estimation in a cox proportional hazards cure model. *Biometrics*, 56(1):227–236.

Tsodikov, A. D., Yakovlev, A. Y., and Asselain, B. (1996). *Stochastic models of tumor latency and their biostatistical applications*, volume 1. World Scientific.

Wang, L., Du, P., and Liang, H. (2012). Two-component mixture cure rate model with spline estimated nonparametric components. *Biometrics*, 68(3):726–735.

Wang, L., McMahan, C. S., Hudgens, M. G., and Qureshi, Z. P. (2016a). A flexible, computationally efficient method for fitting the proportional hazards model to interval-censored data. *Biometrics*, 72(1):222–231.

Wang, P., Zhao, H., and Sun, J. (2016b). Regression analysis of case k interval-censored failure time data in the presence of informative censoring. *Biometrics*, 72(4):1103–1112.

Wang, S., Wang, C., and Sun, J. (2021). An additive hazards cure model with informative interval censoring. *Lifetime Data Analysis*, 27:244–268.

Wang, Y. and Yu, Z. (2021). A kernel regression model for panel count data with time-varying coefficients. *Statistica Sinica*, 31(4):1707–1725.

Wang, Y. and Yu, Z. (2022). A kernel regression model for panel count data with nonparametric covariate functions. *Biometrics*, 78(2):586–597.

Weiner, M. W., Veitch, D. P., Aisen, P. S., Beckett, L. A., Cairns, N. J., Cedarbaum, J., Green, R. C., Harvey, D., Jack, C. R., Jagust, W., et al. (2015). 2014 update of the alzheimer’s disease neuroimaging initiative: a review of papers published since its inception. *Alzheimer’s & dementia*, 11(6):e1–e120.

Weiner, M. W., Veitch, D. P., Aisen, P. S., Beckett, L. A., Cairns, N. J., Green, R. C., Harvey, D., Jack Jr, C. R., Jagust, W., Morris, J. C., et al. (2017a). The alzheimer’s disease neuroimaging initiative 3: Continued innovation for clinical trial improvement. *Alzheimer’s & Dementia*, 13(5):561–571.

Weiner, M. W., Veitch, D. P., Aisen, P. S., Beckett, L. A., Cairns, N. J., Green, R. C., Harvey, D., Jack Jr, C. R., Jagust, W., Morris, J. C., et al. (2017b). Recent publications from the alzheimer’s disease neuroimaging initiative: Reviewing progress toward improved ad clinical trials. *Alzheimer’s & Dementia*, 13(4):e1–e85.

Xie, Y. and Yu, Z. (2021). Mixture cure rate models with neural network estimated nonparametric components. *Computational Statistics*, 36(4):2467–2489.

Xu, J. and Peng, Y. (2014). Nonparametric cure rate estimation with covariates. *Canadian Journal of Statistics*, 42(1):1–17.

Yu, M., Feng, Y., Duan, R., and Sun, J. (2022). Regression analysis of multivariate interval-censored failure time data with informative censoring. *Statistical Methods in Medical Research*, 31(3):391–403.

Zeng, D. and Lin, D. Y. (2006). Efficient estimation of semiparametric transformation models for counting processes. *Biometrika*, 93(3):627–640.

Zeng, D., Mao, L., and Lin, D. (2016). Maximum likelihood estimation for semiparametric transformation models with interval-censored data. *Biometrika*, 103(2):253–271.

Zhao, X., Wu, Y., and Yin, G. (2017). Sieve maximum likelihood estimation for a general class of accelerated hazards models with bundled parameters. *Bernoulli*, 23(4B):3385–3411.

Zhou, J., Zhang, J., and Lu, W. (2018). Computationally efficient estimation for the generalized odds rate mixture cure model with interval-censored data. *Journal of Computational and Graphical Statistics*, 27(1):48–58.

Zhou, Q., Hu, T., and Sun, J. (2017). A sieve semiparametric maximum likelihood approach for regression analysis of bivariate interval-censored failure time data. *Journal of the American Statistical Association*, 112(518):664–672.